ResearchGate

See discussions, stats, and author profiles for this publication at: https://www.researchgate.net/publication/272152661

Evidence for an extraterrestrial impact 12,900 years ago that contributed to the megafaunal extinctions and the Younger Dryas cooling

Article · January 2007

CITATIONS
106

READS
4,832

10 authors, including:

Allen West
Comet Research Group
91 PUBLICATIONS **2,195** CITATIONS
SEE PROFILE

James P Kennett
University of California, Santa Barbara
1,708 PUBLICATIONS **26,878** CITATIONS
SEE PROFILE

Lucía Becker
University Foundation San Pablo CEU
100 PUBLICATIONS **3,307** CITATIONS
SEE PROFILE

Ted E. Bunch
Retired
264 PUBLICATIONS **6,205** CITATIONS
SEE PROFILE

Some of the authors of this publication are also working on these related projects:

Project
Channel Islands Archaeology and Historical Ecology View project

Project
Maritime Dispersals in Deep Human History View project

All content following this page was uploaded by Allen West on 12 February 2020.

The user has requested enhancement of the downloaded file.

Evidence for an extraterrestrial impact 12,900 years ago that contributed to the megafaunal extinctions and the Younger Dryas cooling

R. B. Firestone[a,b], A. West[c], J. P. Kennett[d], L. Becker[e], T. E. Bunch[f], Z. S. Revay[g], P. H. Schultz[h], T. Belgya[g], D. J. Kennett[i], J. M. Erlandson[i], O. J. Dickenson[j], A. C. Goodyear[k], R. S. Harris[h], G. A. Howard[l], J. B. Kloosterman[m], P. Lechler[n], P. A. Mayewski[o], J. Montgomery[j], R. Poreda[p], T. Darrah[p], S. S. Que Hee[q], A. R. Smith[a], A. Stich[r], W. Topping[s], J. H. Wittke[f], and W. S. Wolbach[r]

[a]Lawrence Berkeley National Laboratory, Berkeley, CA 94720; [c]GeoScience Consulting, Dewey, AZ 86327; [d]Department of Earth Sciences and [e]Institute of Crustal Studies, University of California, Santa Barbara, CA 93106; [f]Northern Arizona University, Flagstaff, AZ 86011; [g]Institute for Isotope and Surface Chemistry, H-1525, Budapest, Hungary; [h]Department of Geological Sciences, Brown University, Providence, RI 02912; [i]Department of Anthropology and Museum of Natural and Cultural History, University of Oregon, Eugene, OR 97403; [j]Eastern New Mexico University, Portales, NM 88130; [k]South Carolina Institute of Archaeology and Anthropology, University of South Carolina, Columbia, SC 29208; [l]Restoration Systems, LLC, Raleigh, NC 27604; [m]Rozenstraat 85, 1018 NN, Amsterdam, The Netherlands; [n]Bureau of Mines and Geology, University of Nevada, Reno, NV 89557; [o]Climate Change Institute, University of Maine, Orono, ME 04469; [p]University of Rochester, Rochester, NY 14627; [q]Department of Environmental Health Sciences, University of California, Los Angeles, CA 90095; [s]P.O. Box 141, Irons, MI 49644; and [r]Department of Chemistry, DePaul University, Chicago, IL 60614

Communicated by Steven M. Stanley, University of Hawaii at Manoa, Honolulu, HI, July 26, 2007 (received for review March 13, 2007)

A carbon-rich black layer, dating to ≈12.9 ka, has been previously identified at ≈50 Clovis-age sites across North America and appears contemporaneous with the abrupt onset of Younger Dryas (YD) cooling. The *in situ* bones of extinct Pleistocene megafauna, along with Clovis tool assemblages, occur below this black layer but not within or above it. Causes for the extinctions, YD cooling, and termination of Clovis culture have long been controversial. In this paper, we provide evidence for an extraterrestrial (ET) impact event at ≅12.9 ka, which we hypothesize caused abrupt environmental changes that contributed to YD cooling, major ecological reorganization, broad-scale extinctions, and rapid human behavioral shifts at the end of the Clovis Period. Clovis-age sites in North American are overlain by a thin, discrete layer with varying peak abundances of (*i*) magnetic grains with iridium, (*ii*) magnetic microspherules, (*iii*) charcoal, (*iv*) soot, (*v*) carbon spherules, (*vi*) glass-like carbon containing nanodiamonds, and (*vii*) fullerenes with ET helium, all of which are evidence for an ET impact and associated biomass burning at ≈12.9 ka. This layer also extends throughout at least 15 Carolina Bays, which are unique, elliptical depressions, oriented to the northwest across the Atlantic Coastal Plain. We propose that one or more large, low-density ET objects exploded over northern North America, partially destabilizing the Laurentide Ice Sheet and triggering YD cooling. The shock wave, thermal pulse, and event-related environmental effects (e.g., extensive biomass burning and food limitations) contributed to end-Pleistocene megafaunal extinctions and adaptive shifts among PaleoAmericans in North America.

comet | iridium | micrometeorites | nanodiamonds | spherules

A carbon-rich black layer, dating to ≅12.9 ka (12,900 calendar years B.P.) (1), has been identified by C. V. Haynes, Jr. (2), at >50 sites across North America as black mats, carbonaceous silts, or dark organic clays [supporting information (SI) Fig. 5]. The age of the base of this black layer coincides with the abrupt onset of Younger Dryas (YD) cooling, after which there is no evidence for either *in situ* extinct megafaunal remains or Clovis artifacts. Increasing evidence suggests that the extinction of many mammalian and avian taxa occurred abruptly and perhaps catastrophically at the onset of the YD, and this extinction was pronounced in North America where at least 35 mammal genera disappeared (3), including mammoths, mastodons, ground sloths, horses, and camels, along with birds and smaller mammals. At Murray Springs, AZ, a well known Clovis site, mammoth bones and Clovis-age stone tools lie directly beneath the black layer where, as described by Haynes (4): "[T]he sudden extinction of the Pleistocene megafauna would be dramatically revealed by explaining that all were gone an instant before the black mat was deposited."

The cause of this extinction has long been debated and remains highly controversial due, in part, to the limitations of available data but also because the two major competing hypotheses, human overkill (5) and abrupt cooling (6), fall short of explaining many observations. For example, Grayson and Meltzer (7) summarized serious problems with the overkill hypothesis, such as the absence of kill sites for 33 genera of extinct mammals, including camels and sloths. In addition, although abrupt cooling episodes of magnitudes similar to the YD occurred often during the past 80 ka, none are known to be associated with major extinctions. The possibility of pandemic disease also has been suggested (8), but there is no evidence for that in the Pleistocene record. Thus, the end-Pleistocene extinction event is unique within the late Quaternary and is unlikely to have resulted only from climatic cooling and human overkill. The extinctions were too broad and ecologically deep to support those hypotheses.

Extraterrestrial (ET) catastrophes also have been proposed. For example, LaViolette (9) suggested that a large explosion in our galactic core led to the extinctions. Brakenridge (10) postulated that a supernova killed the megafauna and caused the worldwide deposition of the black layer. Clube and Napier (11) proposed multiple encounters with remnants of the mega comet progenitor of the Taurid meteor stream and Comet Encke. Although ET events have long been proposed as a trigger for mass extinctions, such as at the K/T (≈65 Ma) (12) and P/T (≈250 Ma) (13), there has been no compelling evidence linking impacts to the late Pleistocene megafaunal extinctions and YD cooling.

In the 1990s, W. Topping (14) discovered magnetic microspherules and other possible ET evidence in sediment at the Gainey

Author contributions: R.B.F., A.W., J.P.K., L.B., and W.T. designed research; R.B.F., A.W., J.P.K., L.B., T.E.B., Z.S.R., P.H.S., D.J.K., J.M.E., O.J.D., A.C.G., R.S.H., G.A.H., J.B.K., P.L., P.A.M., J.M., R.P., T.D., S.S.Q.H., A.R.S., A.S., W.T., J.H.W., and W.S.W. performed research; R.B.F., A.W., J.P.K., L.B., T.E.B., Z.S.R., T.B., D.J.K., O.J.D., A.C.G., G.A.H., J.B.K., P.L., J.M., R.P., S.S.Q.H., W.T., J.H.W., and W.S.W. contributed new reagents/analytic tools; R.B.F., A.W., J.P.K., L.B., T.E.B., Z.S.R., P.H.S., D.J.K., J.M.E., R.S.H., G.A.H., P.A.M., R.P., T.D., S.S.Q.H., A.R.S., A.S., W.T., J.H.W., and W.S.W. analyzed data; and R.B.F., A.W., J.P.K., and P.H.S. wrote the paper.

The authors declare no conflict of interest.

Freely available online through the PNAS open access option.

Abbreviations: YD, Younger Dryas; YDB, YD boundary; ET, extraterrestrial.

[b]To whom correspondence should be addressed. E-mail.com rbfirestone@lbl.gov.

This article contains supporting information online at www.pnas.org/cgi/content/full/0706977104/DC1.

© 2007 by The National Academy of Sciences of the USA

Table 1. Information about the YDB research sites, along with concentrations of selected YDB markers

Clovis-age YDB Sites	Date, ka	Misc. markers	Carbon: Spherules #/kg	Magnetic microspherules: #/kg	Magnetic microspherules: FeO, %	Magnetic microspherules: TiO_2, %	Magnetic grains: g/kg	Magnetic grains: H_2O	Magnetic grains: FeO, %	Magnetic grains: TiO_2	Magnetic grains: Ni, ppm	Magnetic grains: IrM, ppb	Bulk: IrB, ppb
Gainey, MI	≈12.4	AGC	1,232	2,144	41	25	3.2	3.2	14	1.6	54	<2	<0.5
Murray Springs, AZ	12.99	AKGCFPSB	0	109			2.6	5.1	21	16	40	<1	2.3
Blackwater Draw, NM	12.98	AKGCFPB	0	768	56	33	2.1	1.5	27	8.1	256	24	2.3
Chobot, AB	≈13	AGCB	11	578			1.9	5.0	14	0.9			
Wally's Beach, AB	12.97	AK	—	6			7.8	1.6	41	8.3	190	51	<1
Topper, SC	<13.5	AG	2	97			1.1	0.7	25	49	440	2	<1
Lommel, Belgium	12.94	ACB	0	16	14	67	0.8	0.8	23	21	23	117	<1
Morley Drumlin, AB	≈13	GCB	16	1,020	60	29	9.9	3.7	14	1.4	240	<0.1	
Daisy Cave, CA	13.09	GCFPB	>0	>0			>0						<1
Lake Hind, MB	12.76	GCB	184	0			0.3						3.8
Carolina Bays, Min		GCFS	142	20			0.5	0.3	18	21		<1	0.5
Carolina Bays, Max			1,458	205			17	1.3	26	34	<200	15	3.8

Radiocarbon ages are calibrated. More site age information is in SI Table 2. Percentages are by weight. A, artifacts from Clovis or contemporaries; K, megafaunal kill-site; G, glass-like carbon; C, charcoal; F, fullerenes with ET He-3; S, soot; P, polycylic aromatic hydrocarbons; B, black mat; Ni, nickel in magnetic fraction; IrM, Ir in magnetic fraction; IrB, Ir in bulk sediment. No measurable Ir was found outside the YDB. Ir uncertainties are ±10% at 117 ppb and ±90% at 0.5 ppb. Geochemical values are less than ±20%.

PaleoAmerican site in Michigan (see also ref. 15), and Lougheed (16) and Bi (17) reported that late Pleistocene glacial drift contained similar cosmic spherules. We now report substantial additional data from multiple, well dated stratigraphic sections across North America supporting a major ET airburst or collision near 12.9 ka. Directly beneath the black mat, where present, we found a thin, sedimentary layer (usually <5 cm) containing high concentrations of magnetic microspherules and grains, nanodiamonds, iridium (Ir) at above background levels, and fullerenes containing ET helium. These indicators are associated with charcoal, soot, carbon spherules, and glass-like carbon, all of which suggest intense wildfires. Most of these markers are associated with previously recorded impacts, but a few are atypical of impact events. We identify this layer as the YD boundary (YDB), and we refer to this incident as the YD event.

At the sites studied, independent radiocarbon (1) and optically stimulated luminescence dates that tend to cluster near 13 ka were used to establish the age of the YDB. For example, the end-Clovis stratum (the YDB) is well dated at Murray Springs, AZ, (eight dates averaging 10,890 ^{14}C yr or calendar 12.92 ka) and the nearby Lehner site (12 dates averaging 10,940 ^{14}C yr or 12.93 calendar ka). Haynes (2) correlated the base of the black mat (the YDB) with the onset of YD cooling, dated to 12.9 ka in the GISP2 ice core, Greenland (see GISP2 chronology in SI Fig. 6) (18). Therefore, we have adopted a calendar age of 12.9 ± 0.1 ka for the YD event.

We propose that the YD event resulted from multiple ET airbursts along with surface impacts. We further suggest that the catastrophic effects of this ET event and associated biomass burning led to abrupt YD cooling, contributed to the late Pleistocene megafaunal extinction, promoted human cultural changes, and led to immediate decline in some post-Clovis human populations (19).

Results

Research Sites. Ten Clovis and equivalent-age sites were selected because of their long-established archeological and paleontological significance, and, hence, most are well documented and dated by previous researchers (see SI Table 2). Two are type-sites where unique PaleoAmerican projectile point styles were first named: the Clovis-point style at Blackwater Draw, NM, and the Gainey-point style at Gainey, MI. Three of the sites are confirmed megafaunal kill sites, and six of 10 have a black mat overlying the YDB. At Blackwater Draw and Murray Springs, the YDB is found directly beneath the black mat and overlying Clovis artifacts with extinct megafaunal remains.

The other sample sites were in and around 15 Carolina Bays, a group of ≈500,000 elliptical lakes, wetlands, and depressions that are up to ≈10 km long and located on the Atlantic Coastal Plain (SI Fig. 7). We sampled these sites because Melton, Schriever (20), and Prouty (21) proposed linking them to an ET impact in northern North America. However, some Bay dates are reported to be >38 ka (22), older than the proposed date for the YD event.

Each of the 10 Clovis-age sites displays a YDB layer (average thickness of 3 cm) that contains a diversity of markers (magnetic microspherules and grains, charcoal, soot, carbon spherules, glass-like carbon, nanodiamonds, and fullerenes with ET helium). The Ir levels are above background in both bulk sediment and magnetic fractions at up to 117 parts per billion (ppb), which is 25% of levels in CI (Ivuna type) chondritic meteorites (23). The YDB also exhibits uranium (U) and thorium (Th) in high concentrations that are up to 25× crustal abundance. At the 15 Bay sites examined, basal sediments and rim sands contain peaks in the same ET assemblage found in the YDB at Clovis sites elsewhere.

YD Event Markers. The various markers are summarized in Table 1 and described in *SI Text*, "Research Sites." Seven representative North American sediment profiles are shown in Fig. 1.

Magnetic microspherules. Magnetic microspherules measuring 10–250 μm peaked in or near the YDB at eight of nine Clovis-age sites and in sediments from five of five Bays tested. Fig. 2 shows representative microspherules from Canada, New Mexico, Michigan, and North Carolina. Several sites also yielded microspherules that appear to be silicates, requiring further analysis. Microspherule abundances average 390 per kilogram and are highest in the north, ranging up to 2,144 per kilogram at Gainey. Analyses from Gainey, the Morley drumlin, and Blackwater Draw found the microspherules to be enriched in titanomagnetite.

Magnetic grains. Magnetic grains measuring 1–500 μm, irregularly shaped and often subrounded, are more abundant than microspherules, and they show a distinct peak in the YDB at all 10 Clovis-age sites and are in all 15 Bays, reaching peaks above the pre-Bay paleosols at four sites. All had lower abundances at other stratigraphic levels. Magnetic grains are mostly dark brown or black, although the magnetic fraction often contains terrestrial silicates with magnetite inclusions. Concentrations of magnetic grains and microspherules vary greatly between YDB sites, averaging 3.4 g/kg, with higher abundances at northern sites, such as Gainey, Chobot, and the Morley drumlin. Lower abundances were found in the Carolinas and the southwestern U.S. Magnetic grains from southern sites and Lommel, along with some YDB microspherules, are enriched in titanomagnetite.

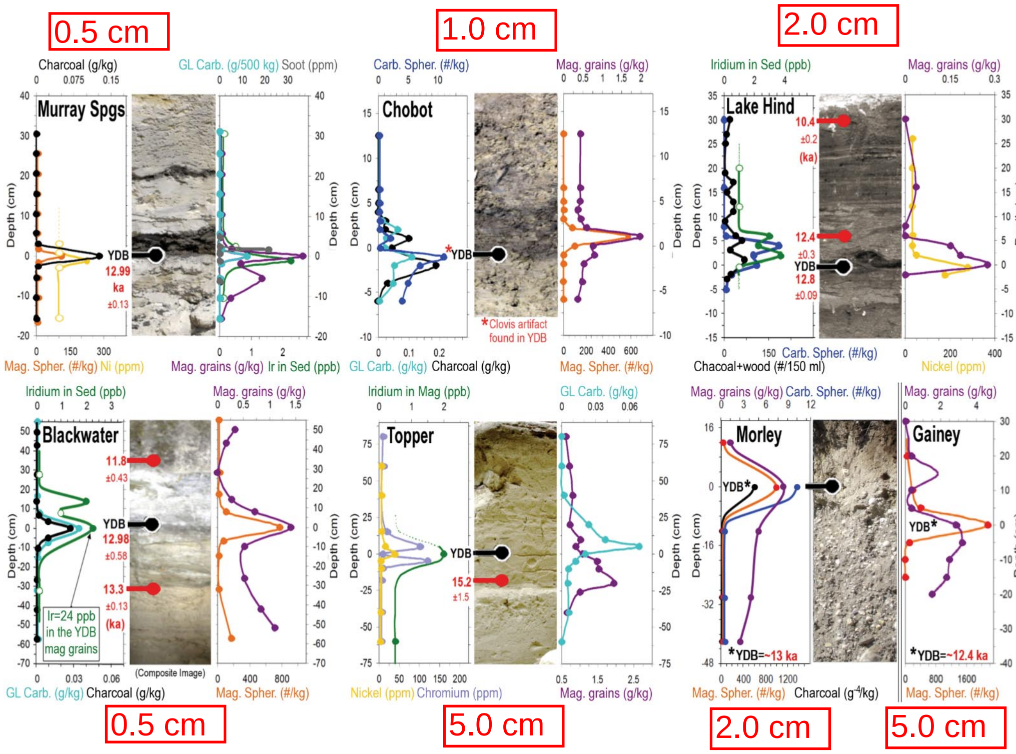

Fig. 1. Sediment profiles for seven sites. Concentrations are shown for magnetic grains, microspherules, charcoal, soot, glass-like carbon, carbon spherules, Ir, Cr, and Ni, which peak mostly in a narrow stratigraphic section spanning only a few hundred years. Ir open circles indicate values below detection, typically <0.5–1 ppb. Ir uncertainties are ±10% at 117 ppb and ±90% at 2 ppb. Cr and Ni are less than ±20%. Keys are color-coded to match the respective curves, and graph points correspond to sampling locations on the photograph. The depth is in centimeters above or below the YDB. The Blackwater Draw image is a composite of three photos. There is no photo for Gainey. A profile for the Belgian site at Lommel is shown in SI Fig. 8. The locations of all sites that were sampled are shown in SI Fig. 9.

Iridium and nickel. YDB sediments, but not the magnetic fractions, are modestly enriched in Ni. For Ir, YDB magnetic grains from seven of 12 sites exhibited a range of 2 (±90%) to 117 (±10%) ppb, and of those seven sites, three also had detectable Ir in the YDB bulk sediment. The highest Ir value is ≈25% that of typical chondrites (455–480 ppb) (24) and >5,000× crustal abundance (0.02 ppb) (25). In 17 measurements at these sites, no Ir was detected in magnetic grains above or below the YDB. For bulk sediment, YDB Ir abundances at five of 12 sites range from 0.5 (±90%) to 3.75 (±50%) ppb. However, the bulk sediment results are near the detection limits of neutron activation analysis, and further testing is required.

Upon retesting aliquots of high-Ir samples, five from nine sites were confirmed, but Ir abundances were below detection in four retests. Sample sizes were small, and variations are likely due to the "nugget effect." In summary, no detectable Ir was found above or below the YDB and black mat at seven sites in 62 samples of both bulk sediments and magnetic grains. Elevated Ir concentrations were found only in the YDB and black mat at nine of 14 widely separated sites (see Fig. 1, Table 1, and SI Table 3).

Charcoal. Charcoal displays peaks in the YDB at eight of nine Clovis-age sites and is present in 15 of 15 Bays, reaching peaks in four Bays with paleosols. The charcoal was identified optically and by SEM based on its distinctive cellular structure and was found in concentrations ranging from 0.06 to 11.63 g/kg.

Soot and polycyclic aromatic hydrocarbons (PAHs). Observed at the K/T boundary (26) and distinguished by its aciniform morphology (see SI Fig. 10) (27), soot forms only in flames through direct condensation of carbon from the gas phase. Soot was identified by using SEM imaging and quantified by particle size analysis and weighing.

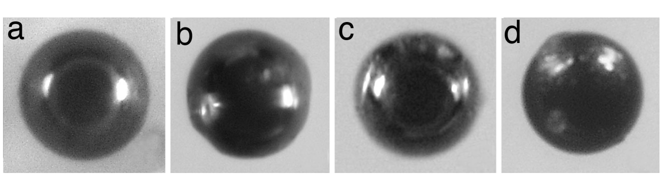

Fig. 2. High-titanomagnetite microspherules from Blackwater Draw, NM (120 μm) (*a*); Chobot, AB, Canada (150 μm) (*b*), Gainey, MI (90 μm) (*c*), and Howard Bay, NC (100 μm) (*d*).

Of eight sites examined, soot was observed only in the YDB at two sites, Murray Springs (21 ± 7 ppm) and Bay T13 (1,969 ± 167 ppm), where preservation possibly resulted from anoxic burial conditions. In addition, the combustion of wood at very high temperatures produces diagnostic PAHs. High-temperature PAHs, which were found at the K/T boundary (28), are present in the YDB, but not above or below it at each of three sites analyzed (Daisy Cave, Murray Springs, and Blackwater Draw), suggesting that intense fires occurred at these locations.

Carbon spherules. Carbon spherules (0.15–2.5 mm) are black, highly vesicular, subspherical-to-spherical objects (Fig. 3). SEM analyses show them to have cracked and patterned surfaces, a thin rind, and honeycombed (spongy) interiors. SEM/energy dispersive spectrometer and microprobe analyses show that the spherules are dominantly carbon (>75%), with no evidence of seed-like morphology or cellular plant structure, as in charcoal. They were found in 13 of 15 Bays and only in the YDB at six of nine Clovis-age sites in concentrations up to ≈1,500 per kilogram. In addition, we recovered them from one of four modern forest fires (see *SI Text*, "Research Sites"), confirming that they can be produced by intense heat in high-stand wildfires. At the P/T boundary, Miura[t] discovered carbon spherules up to 90 wt% C and up to 20 μm in size, which he attributes to a controversial cosmic impact ≈250 Ma. More recently, Rösler *et al.*[u] reported finding carbon spherules from undated sediment across Europe, and these appear identical to spherules from the YDB layer. The authors report that they contain fullerenes and nanodiamonds, the latter of which are extraordinarily rare on Earth but are found in meteorites and at ET impact sites (29), leading those authors to propose an ET association for the carbon spherules.

Fullerenes and ET helium. Of four sites analyzed, fullerenes with ET helium, which are associated with meteorites and ET impacts (30), were present in YDB sediments at three Clovis-age sites (Blackwater, Murray Springs, and Daisy Cave). In Bay M33, they

[t]Miura, Y., 37th Annual Lunar and Planetary Science Conference, March 13–17, 2006, League City, TX, Vol. 2441, pp. 1–2 (abstr.).

[u]Rösler, W., Hoffmann, V., Raeymaekers, B., Yang, Z. Q., Schryvers, D., Tarcea, N. (2006) First International Conference on Impact Cratering in the Solar System, May 7–12, 2006, Noordwijk, The Netherlands, abstr. 295464.

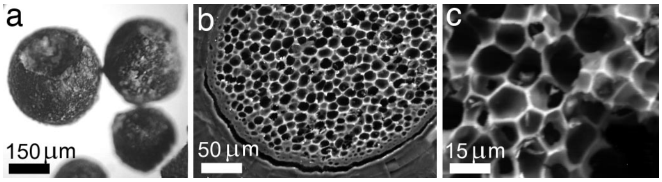

Fig. 3. Low-density carbon spherules are shown whole from the Chobot site (*a*), sectioned and by SEM from Bay T13 (*b*), and at high magnification by SEM from Bay B14 (*c*).

also were found in glass-like carbon with an ET helium ratio that is 84 times that of air. By comparison, the ratio of the Tagish Lake meteorite was 90 times that of air.

Glass-Like Carbon. Pieces up to several cm in diameter (Fig. 4) were found associated with the YDB and Bays, and their glassy texture suggests melting during formation, with some fragments grading into charcoal. Continuous flow isotope ratio MS analysis of the glass-like carbon from Carolina Bay M33 reveals a composition mainly of C (71%) and O (14%). Analysis by ^{13}C NMR of the glass-like carbon from Bay M33 finds it to be 87 at.% (atomic percent) aromatic, 9 at.% aliphatic, 2 at.% carboxyl, and 2 at.% ether, and the same sample contains nanodiamonds, which are inferred to be impact-related material (see SI Fig. 11). Concentrations range from 0.01 to 16 g/kg in 15 of 15 Bays and at nine of nine Clovis-age sites in the YDB, as well as sometimes in the black mat, presumably as reworked material. Somewhat similar pieces were found in four modern forest fires studied (see *SI Text*, "Research Sites").

Quantities for selected markers are shown in Table 1, and abundances of all markers are given in SI Table 4.

Discussion

Age of the YDB. The YDB at the 10 Clovis- and equivalent-age sites has been well dated to ≈12.9 ka, but the reported ages of the Carolina Bays vary. However, the sediment from 15 Carolina Bays studied contain peaks in the same markers (magnetic grains, microspherules, Ir, charcoal, carbon spherules, and glass-like carbon) as in the YDB at the nearby Topper Clovis site, where this assemblage was observed only in the YDB in sediments dating back >55 ka. Therefore, it appears that the Bay markers are identical to those found elsewhere in the YDB layers that date to 12.9 ka. Although the Bays have long been proposed as impact features, they have remained controversial, in part because of a perceived absence of ET-related materials. Although we now report that Bay sediments contain impact-related markers, we cannot yet determine whether any Bays were or were not formed by the YD event.

Peaks in Markers. We investigated whether peaks in YDB markers might be attributed to terrestrial processes. The 25 sites examined represent a wide range of depositional environments (fluvial, lacustrine, eolian, alluvial, colluvial, and glacial), soil conditions (aerobic/well drained to anaerobic/saturated), sediment composition (dense clay to gravelly sand), climatic regimes (semiarid to periglacial), and biomes (grasslands to forests). The presence of identical markers found under such a wide range of conditions argues against formation by terrestrial processes and is consistent with an impact origin. We also examined whether the YDB might represent an interval of reduced deposition, allowing the accretion of interplanetary dust particles enriched in ET markers, such as Ir, Ni, and ET helium. At Blackwater Draw, based on 24 calibrated ^{14}C dates from 13.30 to 10.99 ka, Haynes (31, 32) suggested that any hiatus at the level representing the YDB most likely lasted less than a decade, which is insufficient to have produced a local Ir bulk sediment level that is >100× crustal abundance. Furthermore, abundances of microspherules and magnetic grains decrease with increasing distance from the Great Lakes region (see SI Fig. 12). This nonrandom distribution is unlikely to be due to terrestrial factors or interplanetary dust storms, but it is consistent with airburst/impacts over northern North America.

Fig. 4. Examples of glass-like carbon from Gainey, Bay M31, and Topper.

Magnetic Microspherules and Grains. High concentrations of microspherules (glass, clinopyroxene, spinel, or metallic) are accepted as evidence for at least 11 older ET impact events (33). Alternately, microspherules are sometimes associated with volcanism, but when YDB microspherules were analyzed by SEM/x-ray fluorescence and compared with known cosmic and volcanic microspherules (34, 35), they appear to be nonvolcanic in origin. Analysis suggests an ET origin, but because of high titanium (Ti) concentrations, the microspherules differ from typical meteoritic ones.

The magnetic grains and microspherules are anomalously enriched in Ir and Ti (see Table 1 and SI Table 5) and are enriched in water (up to 28 at.%), especially at northern sites. TiO_2/FeO ratios of microspherules (0.48 ratio) and magnetic grains (0.76) are 4- to 250-fold higher than Alaskan terrestrial magnetite (<0.12 ratio in 347 samples) (36), crustal abundance (0.13) (25), CI chondrites (0.003) (23), and K/T impact layers (0.07) (12). These ratios and the similarity in composition of YDB magnetic microspherules and magnetic grains (e.g., high Ti) from many sites across North America cannot be explained at this time, but the YDB abundance of microspherules and magnetic grains most likely resulted from the influx of ejecta from an unidentified, unusually Ti-rich, terrestrial source region and/or from a new and unknown type of impactor.

Carbon-Rich Markers. At Murray Springs, Haynes (37) first reported the presence of glass-like or "vitreous" carbon in the black mat. In addition, he chemically analyzed the black mat layer, concluding that it most likely resulted from the decomposition of charred wood and/or a prolonged algal bloom, both of which could result from event-related processes (e.g., climate change and biomass burning). Some black mats have no algal component, only charcoal. The widespread peaks of charcoal in or near the YDB, and their association with soot and polycyclic aromatic hydrocarbons at specific sites, provide strong evidence for extensive wildfires. We propose that glass-like carbon, carbon spherules, and nanodiamonds were produced in the YDB by high temperatures resulting from the impact and associated biomass burning.

Ir Anomaly. Ir concentrations in sediments and ocean cores are high for many accepted impact events, such as for the K/T and Chesapeake Bay (≈36 Ma) (38). However, Ir values in the YDB bulk sediment are lower than at many K/T sites (e.g., 9.1 ppb at Gubbio, Italy) (12), suggesting much less Ir in the YD impactor. The evidence indicates an Ir anomaly in both the YDB bulk sediment and the magnetic fraction; however, for Ir in the bulk sediment, the level of uncertainty remains high (±50–90%), in contrast to the magnetic fraction, where values have higher certainty (up to ±10%), and are, therefore, more compelling. In 169 measurements at 14 sites up to ≈9,200 km apart, Ir was detected only in the YDB sediments, YDB magnetic fraction, and the black mat. Ir never was detected above or below these layers, lessening concerns about the high uncertainties, while providing strong evidence that Ir concentrations are above background in the YDB or black mat. The relatively low Ir and Ni peaks associated with the YDB are more consistent with the generally proposed composition of comets and inconsistent with the high-Ir content typical of most stony, nickel–iron, or chondritic meteorites.

Alternately, Ir peaks are found at major geologic boundary layers with no confirmed impacts, and at least some of those Ir concentrations may have resulted from volcanism. However, no major North American volcanic episode is known at 12.9 ka, and, according to Koeberl (39), such events produce Ir abundances of <0.5 ppb, much less than we find in the YDB. Therefore, the high concentrations of Ir do not appear to be of volcanic origin.

We also considered microbial concentration from Ir-rich adjacent sediment, such as occurred in experiments by Dyer *et al.* (40), who cultured microbes in Ir-rich igneous rocks and meteoritic material. However, at all sites analyzed, non-YDB sediment levels of Ir are very low (<0.1 ppb and possibly <0.02 ppb) and are insufficient to account for Ir levels up to 5,000× crustal abundance. Given the association of high Ir with a suite of other event-related markers, an ET connection is more plausible.

Ice Core Evidence. Large increases in Ir and Pt occurred during the Younger Dryas as recorded in the GRIP (Greenland) ice core by Gabrielli *et al.* (41), who attributed these increases to increased cosmic input. Although sample resolution in the ice core was too low to permit us to specifically link the onset of these increased fluxes with the timing of the YD event, the evidence is consistent with the YD event.

As evidence for biomass burning, Mayewski *et al.* (42, 43) reported large ammonium and nitrate spikes in the Greenland GISP2 ice core at the onset of the YD. These GISP2 data are consistent with strong geochemical evidence in the GRIP ice core for massive biomass burning at the YD onset, especially a major ammonium spike, in association with peaks in nitrate, nitrite, formate, oxalate, and acetate (44). Altogether, the YD onset was one of the most robust intervals of biomass burning inferred from the Greenland ice cores, although the source of this burning signal must have been far more remote than sources today, because much of the modern forested Arctic region was then covered by ice. The cause of this biomass burning is consistent with the YD event.

Radioactive Elements. Some megafaunal bones in the YDB are highly radioactive relative to other stratigraphic intervals, as occurred for some bones at the K/T boundary (see SI Figs. 13 and 14). In addition, high concentrations of U and Th were found in the YDB sediment at six of six Clovis-age sites analyzed and in four of four Bays with a paleosol, just as were found in the impact layers at Chesapeake Bay (38) and the K/T (see SI Fig. 15) (45). Because the heavy minerals, zircon, monazite, and garnet, along with Ti-rich minerals, such as titanite, ilmenite, and rutile, sometimes contain high concentrations of U and Th, we investigated whether lag deposits of those minerals might be the source of high radioactivity. We conclude that lag deposits may explain the high YDB radioactivity at some sites but not at others. Ilmenite, rutile, and titanite are possible carriers given that they comprise up to ≈2% of all sediments, but zircon, monazite, and garnet are unlikely, because they represent <0.1% each (see SI Figs. 16 and 17). The elevated levels of U and Th may result from multiple processes related to the impacts/airbursts, including formation of lag deposits, as well as the dispersal of ejecta from the impactor and/or the target area.

Nature of the Event. The evidence points to an ET event with continent-wide effects, especially biomass burning, but the size, density, and composition of the impactor are poorly understood. Even so, current data suggest that this impactor was very different from well studied iron, stony, or chondritic impactors (e.g., at the K/T boundary). The evidence is more consistent with an impactor that was carbon-rich, nickel–iron-poor, and therefore, most likely a comet. Although the current geologic and geochemical evidence is insufficient to fully understand impact dynamics, we can offer speculation for future work.

Toon *et al.* (46) suggest that an impact capable of continent-wide damage requires energy of 10^7 megatons, equivalent to an impact by a >4-km-wide comet (figure 1 in ref. 46). Although an impactor that size typically leaves an obvious large crater, no such late Pleistocene crater has been identified. The lack of a crater may be due to prior fragmentation of a large impactor, thereby producing multiple airbursts or craters. Hypervelocity oblique impact experiments (P.H.S., unpublished data) indicate that a low-impedance surface layer, such as an ice sheet, can markedly reduce modification of the underlying substrate if the layer is equal to the projectile's diameter. These results suggest that if multiple 2-km objects struck the 2-km-thick Laurentide Ice Sheet at <30°, they may have left negligible traces after deglaciation. Thus, lasting evidence may have been limited to enigmatic depressions or disturbances in the Canadian Shield (e.g., under the Great Lakes or Hudson Bay), while producing marginal or no shock effects and dispersing fine debris composed of the impactor, ice-sheet detritus, and the underlying crust.

Toon *et al.* (46) also noted that if airbursts explode with energy of 10^7 megatons at optimum height, they will cause blast damage over an area the size of North America that is equivalent to a ground impact of 10^9 megatons (figure 5 in ref. 46). Such airbursts effectively couple the impactor's kinetic energy with the atmosphere or surface (47, 48), producing devastating blast waves well above hurricane force ($70\ m \cdot s^{-1}$) (46). In 1908, at Tunguska, Siberia, a object <150 m in diameter, either a carbonaceous asteroid or a small, burned-out comet, produced a <15-megaton airburst with an intense fireball (10^7 °C) that scorched ≈200 km^2 of trees and leveled ≈2,000 km^2 of forest yet produced no crater or shock metamorphism (49). A debris shower from a heavily fragmented comet (11) would have produced an airburst barrage that was similar to, although exponentially larger than Tunguska, while causing continent-wide biomass burning and ice-sheet disruption, but again possibly, without typical cratering.

Environmental Effects. The YD event would have created a devastating, high-temperature shock wave with extreme overpressure, followed by underpressure, resulting in intense winds traveling across North America at hundreds of kilometers per hour, accompanied by powerful, impact-generated vortices (50–52). In addition, whether single or multiple objects collided with Earth, a hot fireball would have immersed the region near the impacts and would have been accentuated if the impact angles were oblique (46, 53). For comparison, Svetsov (48) calculated that a Tunguska-sized airburst would immerse the ground with a radiation flux severe enough to ignite 200 km^2 of forest within seconds. Thus, multiple, larger airbursts would have ignited many thousands of square kilometers. At greater distances, the reentry of high-speed, superheated ejecta would have induced extreme wildfires (53), which would have decimated forests and grasslands, destroying the food supplies of herbivores and producing charcoal, soot, toxic fumes, and ash. The number of ET airbursts or impacts necessary to induce the continent-wide environmental collapse at 12.9 ka is unknown.

Climate. A number of impact-related effects most likely contributed to the abrupt, major cooling at the onset of the YD and its maintenance for >1,000 years. Cooling mechanisms operating on shorter time scales may have included (*i*) ozone depletion, causing shifts in atmospheric systems in response to cooling, with the side-effect of allowing increased deadly UV radiation to reach survivors on the surface (46); (*ii*) atmospheric injection of nitrogen compounds (NO_x), sulfates, dust, soot, and other toxic chemicals from the impact and widespread wildfires (46), all of which may have led to cooling by blockage of sunlight, with the side-effect of diminished photosynthesis for plants and increased chemical toxicity for animals and plants (46); and (*iii*) injection of large amounts of water vapor and ice into the upper atmosphere to form persistent cloudiness and noctilucent clouds, leading to reduced sunlight and surface cooling (46). Although these cooling mechanisms tend to be short-lived, they can trigger longer-term consequences through feedback mechanisms. For example, noctilucent clouds can reduce solar insolation at high latitudes, increasing snow accumulation and causing further cooling in a feedback loop. The largest potential effect would have been impact-related partial destabilization and/or melting of the ice sheet. In the short term, this would have suddenly released meltwater and rafts of icebergs into the North Atlantic and Arctic Oceans, lowering surface-ocean salinity with consequent surface cooling. The longer-term cooling effects largely would have resulted from the consequent weakening of thermohaline circulation in the northern Atlantic (54), sustaining YD cooling for >1,000 years until the feedback mechanisms restored ocean circulation.

Clovis and Megafauna. The impact-related effects would have been devastating for animals and plants. For humans, major adaptive shifts are evident at 12.9 ka, along with an inferred population decline, as subsistence strategies changed because of dramatic ecological change and the extinction, reduction, and displacement of key prey species (55, 56). Many sites indicate that both Clovis people and extinct megafauna were present immediately before the YD event, but, except in rare cases, neither appears in the geologic record afterward. At Murray Springs, butchered, still-articulated mammoth bones, Clovis tools, and a hearth were found buried directly beneath the black mat, indicating that it buried them rapidly (37). YDB markers, including Ir at 51 ppb, occur inside an extinct horse skull at the Wally's Beach Clovis kill-site (57), again suggesting rapid burial following the YD event. It is likely that some now-extinct animals survived in protected niches, only later to become extinct because of insufficient food resources, overhunting, climate change, disease, flooding, and other effects, all triggered or amplified by the YD event.

Conclusions

Our primary aim is to present evidence supporting the YD impact event, a major ET collision over North America at 12.9 ka, which contributed to the YD cooling, the massive extinction of the North American fauna, and major adaptations and population declines among PaleoAmericans. The unique, carbon-rich, YDB layer, coupled with a distinct assemblage of impact tracers, implies isochroneity of the YDB datum layer and thus highlights its utility for correlation and dating of the North American late Pleistocene. These associations, if confirmed, offer the most complete and recent geological record for an ET impact and its effects, such as global climate change and faunal extinction. This evidence also would represent a record of a major ET event having serious, widespread consequences for anatomically modern humans.

Methods

Elemental analyses were performed by using prompt gamma-ray activation analysis, neutron activation analysis, and inductively coupled plasma MS. Microspherules, glass-like carbon, and carbon spherules were analyzed by SEM/x-ray fluorescence. These methods are very standard and discussed further in *SI Text*, "Methods."

We thank C. V. Haynes, Jr., and J. Ballenger (University of Arizona, Tucson, AZ), B. Kooyman and colleagues (University of Calgary, Calgary, BC, Canada), B. Childress and J. Pike-Childress (Bureau of Land Management, Phoenix, AZ), M. Boyd and colleagues (Lakehead University, Thunder Bay, ON, Canada), A. Huston, (Channel Islands National Park, Ventura, CA), J. Johnson (Santa Barbara Museum of Natural History, Santa Barbara, CA), M. Waters and A. Rodriguez (University of North Carolina, Chapel Hill), D. Kimbel (Restoration Systems, LLC), and W. Newell (Restoration Systems, LLC) for providing/collecting samples and/or for access to sites; M. Gifford for help with inductively coupled plasma MS analyses; Henry Wright (University of Michigan, Ann Arbor, MI) and Denise Henry and Terrence Rettig (National Science Foundation, Arlington, VA) for early help and encouragement; J. Talbot (K/T GeoServices, Argyle, TX), B. Cannon (Cannon Microprobe, Seattle, WA), C. J. Eastoe (University of Arizona), J. Edwards (Process NMR Associates, Danbury, CT), E. Hoffman (Activation Laboratories, Ancaster, ON, Canada), J. Feathers and J. Johnson (University of Washington, Seattle, WA), S. Simpson (Becquerel Laboratories, Mississauga, ON, Canada), Philippe Claeys (Vrije Universiteit Brussel, Brussels, Belgium), and J. Southon (University of California, Irvine, CA) for their careful analyses of samples. This work was supported, in part, by U.S. Department of Energy Contract DE-AC02-05CH11231 and National Science Foundation Grants 9986999, OCD-0244201, and ATM-0713769.

1. Taylor R, Haynes CV, Jr, Stuiver M (1996) *Antiquity* 70:515–525.
2. Haynes, CV, Jr (2005) in *Paleoamerican Origins: Beyond Clovis*, eds Bonnichsen R, Lepper BT, Stanford D, Waters MR (Texas A&M Univ Press, College Station, TX), pp 113–132.
3. Grayson D, Meltzer D (2003) *J Arch Sci* 30:585–593.
4. Haynes CV (1998) *Mammoth Trumpet* 13(2):2–6.
5. Mosimann J, Martin P (1975) *Am Scientist* 63:304–313.
6. Guthrie R (2006) *Science* 441:207–209.
7. Grayson D, Meltzer D (2003) *J Arch Sci* 30:585–593.
8. MacPhee R, Marx P (1997) in *Natural Change and Human Impact in Madagascar,* eds Goodman S, Patterson B (Smithsonian Inst Press, Washington, DC), pp 169–217.
9. LaViollete P (1987) *Earth, Moon, Planets* 37:241–286.
10. Brakenridge G (1981) *Icarus* 46:81–93.
11. Clube V, Napier W (1984) *Mon Not R Astronom Soc* 211:953–968.
12. Alvarez L, Alvarez W, Asaro F, Michel H (1980) *Science* 208:1095–1108.
13. Becker L, Poreda RJ, Basu AR, Pope KO, Harrison TM, Nicholson C, Lasky R (2004) *Science* 304:1469–1476.
14. Firestone RB, Topping W (2001) *Mammoth Trumpet* 16(9):1–5.
15. Firestone RB, West A, Warwick-Smith S (2006) *Cycle of Cosmic Catastrophes* (Bear, Rochester, VT), pp 19–35.
16. Lougheed MS (1966) *Ohio J Sci* 66:274–283.
17. Bi D (1993) *Meteoritics* 29:88–93.
18. Alley RB (2000) *Quat Sci Revs* 19:213–226.
19. Goodyear AC (2006) *Curr Res Pleistocene*, 23:100–101.
20. Melton FA, Schriever W (1933) *J Geol* 41:52–56.
21. Prouty WF (1952) *Bull GSA* 63:167–224.
22. Frey DJ (1955) *Ecology* 36(4):762–763.
23. Anders E, Grevesse N (1989) *Geochim Cosmo Acta* 53:197–214.
24. McDonough W, Sun S (1995) *Chem Geol* 120:223–253.
25. Rudnick R, Gao R (2003) *Treatise on Geochemistry,* eds Holland H, Turekian K (Elsevier, Oxford, UK), Vol 3, pp 1–64.
26. Wolbach WS, Lewis RS, Anders E (1985) *Science* 230:167–170.
27. Kroto H (1988) *Science* 242:1139–1145.
28. Venkatesan MI, Dahl J (1989) *Nature* 338:57–60.
29. Gilmour I, Russell SS, Arden JW, Lee MR, Franchi IA, Pillinger CT (1992) *Science* 258:1624–1626.
30. Becker L, Poreda RJ, Bunch TE (2000) *Proc Natl Acad Sci USA* 97:2979–2983.
31. Haynes CV, Jr (1995) *Geoarchaeology* 10(5):317–388.
32. Haynes CV, Jr, Stanford DJ, Jodry M, Dickenson J, Montgomery JL, Shelley PH, Rovner I, Agogino GA (1999) *Geoarchaeology* 14(5):455–470.
33. Simonson B, Glass B (2004) *Annu Rev Earth Planet Sci* 32:329–361.
34. Iyer SD, Prasad MS, Gupta SM, Charan SN, Mukherjee AD (1997) *J Volcanol Geotherm Res* 78:209–220.
35. Wright F, Hodge P, Allen R (1966) *Smithson Astrophys Obs Spec Rep* 228:1–9.
36. Pan K-L, Overstreet WC, Robinson K, Hubert AE, Crenshaw GL (1980) *USGS Professional Publications* 1135:3–22.
37. Haynes CV, Jr (2007) in *Murray Springs: A Clovis Site with Multiple Activity Areas in the San Pedro Valley, Arizona*, eds Haynes CV, Jr, Huckell BB (Univ of Arizona Press, Tucson, AZ), pp 240–249.
38. Bodiselitsch B, Montanari A, Koeberl C, Coccioni R (2004) *Earth Planet Sci Lett* 223:283–302.
39. Huber H, Koeberl C, Egger H (2003) *Geochem J* 37:123–134.
40. Dyer BD, Lyalikova NN, Murray DP, Doyle M, Kolesov GM, Krumbein WE (1989) *Geology* 17(11):1036–1039.
41. Gabrielli P, Barbante C, Plane JM, Varga A, Hong S, Cozzi G, Gaspari V, Planchon FA, Cairns W, Ferrari C, *et al.* (2004) *Nature* 432:1011–1014.
42. Mayewski PA, Meeker LD, Whitlow SI, Twickler MS, Morrison MG, Alley RB, Bloomfield P, Taylor K (1993) *Science* 261:195–197.
43. Mayewski PA, Meeker LD, Twickler MS, Whitlow SI, Yang Q, Lyons WB, Prentice M (1997) *J Geophys Res* 102:26345–26366.
44. Legrand M, De Angelis M (1995) *J Geophys Res* 100:1445–1462.
45. Martinez-Ruiz F, Ortega-Huertas M, Palomo I (1999) *Terra Nova* 11:290–296.
46. Toon OB, Tukco RP, Covey C, Zahnle K, Morrison D (1997) *Rev Geophys* 35:41–78.
47. Schultz PH, Gault DE (1985) *J Geophys Res* 90:3701–3732.
48. Svetsov VV (2002) *Palaeogeogr Palaeoclim Palaeoecol* 185:403–405.
49. Wasson JT (2003) *Astrobiology* 3:163–179.
50. Schultz PH (1992) *J Geophys Res* 97:16183–16248.
51. Barnouin-Jha O, Schultz PH (1996) *J Geophys Res* 101:21099–21115.
52. Wrobel K, Schultz PH, Crawford D (2006) *Meteorit Planet Sci* 41:1539–1550.
53. Schultz PH, D'Hondt S (1996) *Geology* 24:963–967.
54. Broecker WS (2006) *Science* 312:1146–1148.
55. Anderson DG, Faught MK (2000) *Antiquity* 74:507–513.
56. Bamforth DB (2002) *J World Prehistory* 16(1):55–98.
57. Kooyman B, Newman ME, Cluney C, Lobb M, Tolman S, McNeil P, Hills LV (2001) *Am Antiquity* 66:686–691.
58. Boyd M, Running G, Havholm K (2003) *Geoarchaeology* 18:583–607.

Info for Authors | Editorial Board | About | Subscribe | Advertise | Contact

PNAS

Proceedings of the National Academy of Sciences of the United States of America

Firestone *et al*. 10.1073/pnas.0706977104.

Supporting Information

(Use Ctrl + Click to jump to file)

FIGURES:

TEXT:

TABLES:

Fig. 5. The dark line shown above is the black mat (12.9 ka) along the arroyo wall of the Murray Springs Clovis site in Arizona. The YDB markers, including magnetic grains and microspherules, iridium, soot, and fullerenes with ET helium, are present in the few centimeters just below the black mat at the top of the underlying sediment. This lithologic break represents the surface at the end of the Clovis period before the formation of the black mat. Clovis artifacts, a fire pit, and an almost fully articulated skeleton of an adult mammoth were recovered at Murray Springs with the black mat draped conformably over them. Excavations by Vance Haynes, Jr., and colleagues also revealed hundreds of mammoth footprints in the sand infilled by black mat sediments. These footprints and the mammoth skeleton appear to have been preserved by rapid burial after the YDB event (1). No *in situ* Clovis points and extinct megafaunal remains have been recovered from in or above the black mat, indicating that the mammoths (except in isolated cases) and Clovis hunting technology disappeared simultaneously.

1. Haynes CV, Jr (1987) *Centennial Field Guide Volume 1: Cordilleran Section of the Geological Society of America* (Geolog. Soc. Am., Boulder, CO), Vol. 1, pp 23-28.

[Back to Top]

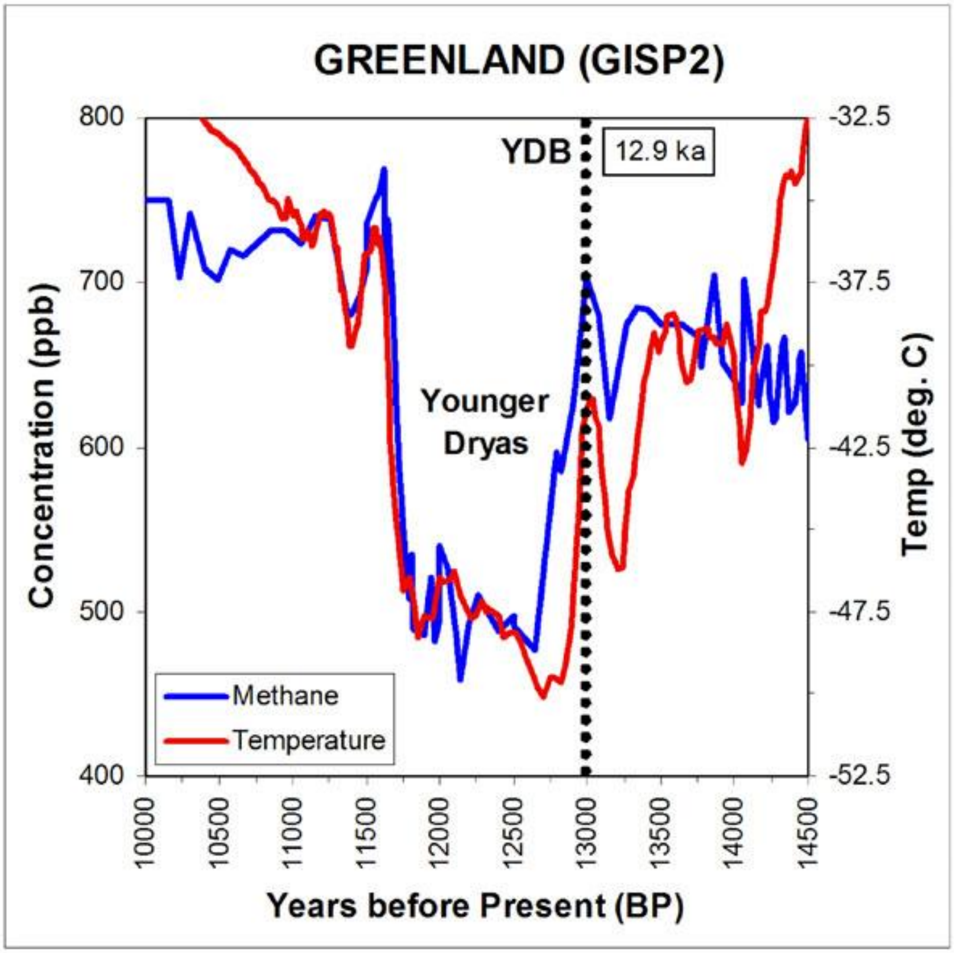

Fig. 6. Clovis and the Younger Dryas. Haynes, in Taylor *et al.* (1), correlated the end of Clovis cultural adaptations with the onset of Younger Dryas cooling and provided end-Clovis ^{14}C dates that have been calibrated to 12.92 ka for Murray Springs and 12.98 ka for Blackwater Draw, two of the sites we analyzed. This graph displays a corresponding date of 12.9 ka for the onset of the YD in Greenland GISP2 ice core data based on paleotemperature analyses (ref. 2, in red) and changes in methane concentrations (ref. 3, in blue). The onset of the YD was marked by a dramatic 8°C drop in Greenland temperature in <150 years with an associated abrupt decrease in atmospheric methane concentrations. We propose that these climatic changes were triggered by the YD event at ≈12.9 ka.

1. Taylor RE, Haynes CV, Stuiver M (1996) *Antiquity* 70:515-525.

2. Alley RB (2000) *Quaternary Sci Rev* 19:213-226.

3. Brook EJ, Harder S, Severinghaus J, Steig EJ, Sucher CM (2000) *Cycles* 14(2):559-572.

[Back to Top]

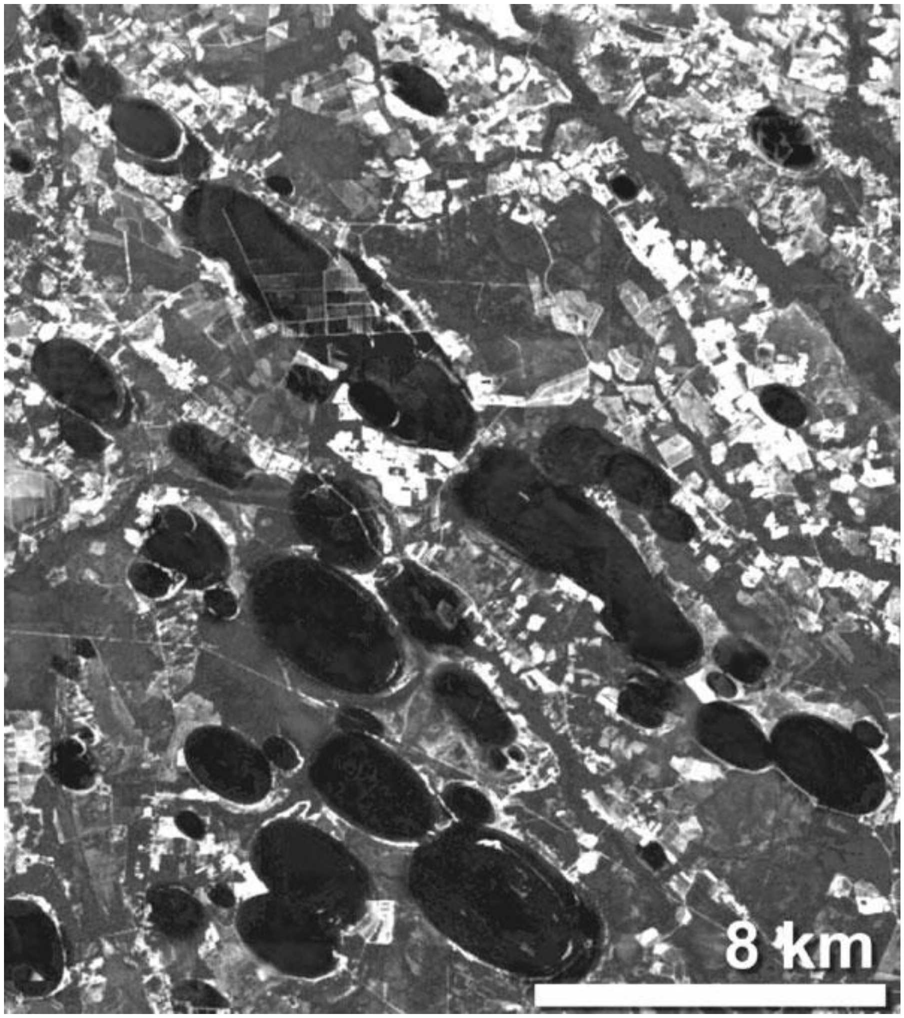

Fig. 7. Aerial photo (U.S. Geological Survey) of a cluster of elliptical and often overlapping Carolina Bays with raised rims in Bladen County, North Carolina. The Bays have been contrast-enhanced and selectively darkened for greater clarity. The largest Bays are several kilometers in length, and the overlapping cluster of them in the center is ≈8 km long. Previous researchers have proposed that the Bays are impact-related features.

[Back to Top]

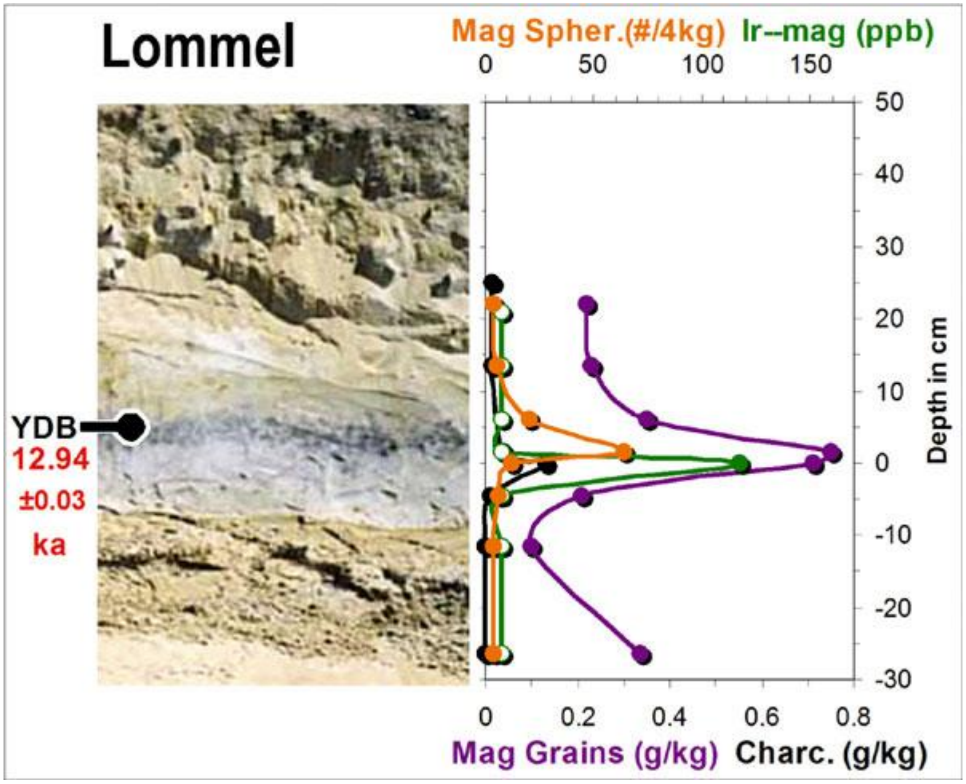

Fig. 8. Lommel (1) is in northern Belgium, near the border with the Netherlands. At 12.94 ka (2), this site was a large late Glacial sand ridge covered by open forest at the northern edge of a marsh. More than 50 archaeological sites in this area indicate frequent visits by the late Magdalenians, hunter-gatherers who were contemporaries of the Clovis culture in North America. Throughout the Bölling-Allerod, eolian sediments known as the Coversands blanketed the Lommel area. Then, just before the Younger Dryas began, a thin layer of bleached sand was deposited and, in turn, was covered by the dark layer marked "YDB" above. That stratum is called the Usselo Horizon and is composed of fine to medium quartz sands rich in charcoal. The dark Usselo Horizon is stratigraphically equivalent to the YDB layer and contains a similar assemblage of impact markers (magnetic grains, magnetic microspherules, iridium, charcoal, and glass-like carbon). The magnetic grains have a high concentration of Ir (117 ppb), which is the highest value measured for all sites yet analyzed. On the other hand, YDB bulk sediment analyses reveal Ir values below the detection limit of 0.5 ppb, suggesting that the Ir carrier is in the magnetic grain fraction. The abundant charcoal in this black layer suggests widespread biomass burning. A similar layer of charcoal, found at many other sites in Europe, including the Netherlands (3), Great Britain, France, Germany, Denmark, and Poland (4), also dates to the onset of the Younger Dryas (12.9 ka) and, hence, correlates with the YDB layer in North America. [Reproduced with permission from Marc De Bie (Copyright 2004).]

1. Hoek WZ (1997) *Veget Hist Archaeobot* 6:197-213.

2. Van Geel B, Coope GR, Vander Hammen T (1989) *Rev Paleont Palyn* 60:25-129.

3. Hoek WZ (1997) *Veget Hist Archaeobot* 6:197-213.

4. Kloosterman JB (1976) *Catastroph Geol* 1(2):57-58.

[Back to Top]

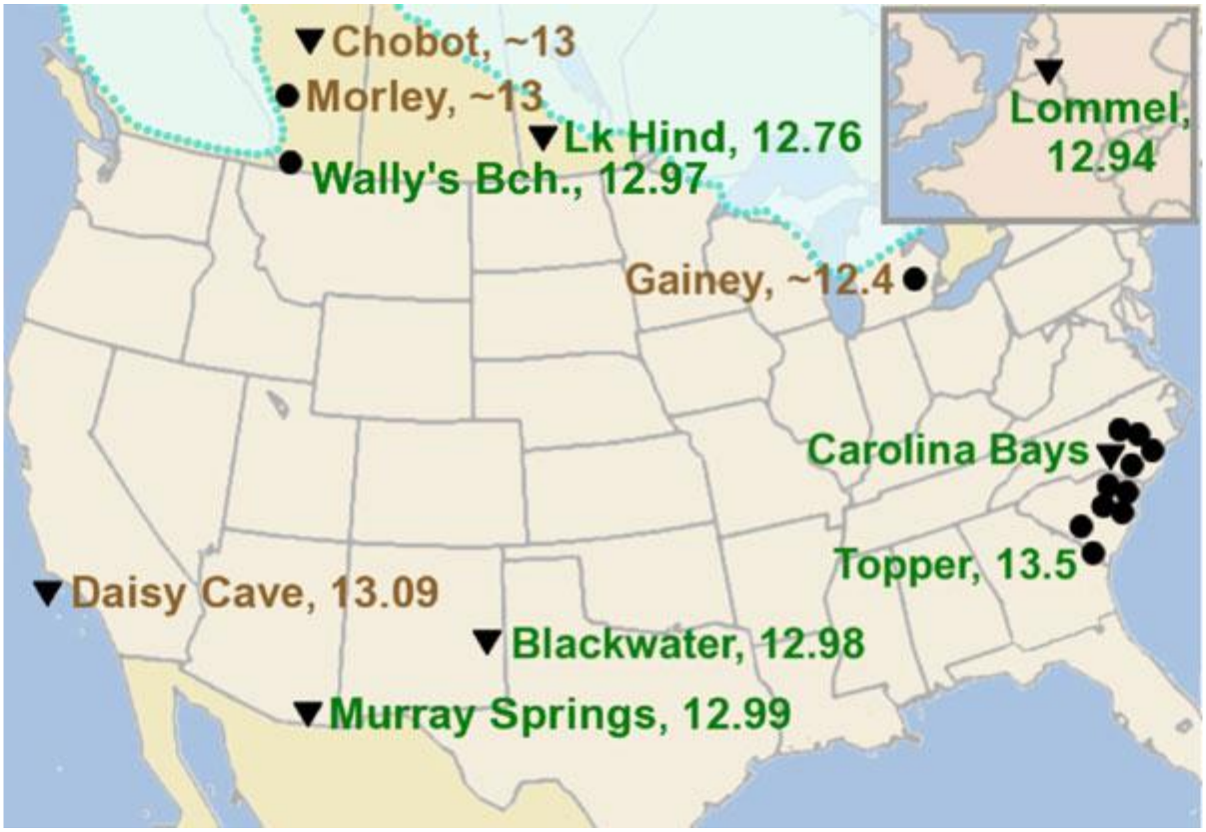

Fig. 9. Research sites with calibrated YDB ages, including Lommel, Belgium, shown in *Inset*. High-Ir sites are shown in green. For the Bays, three of five sediment analyses revealed detectable Ir values, although radiocarbon ages of the Bays are inconsistent. Sediments from sites with no detectable Ir values (<0.5 ppb) are shown in brown. Sites with black mats are marked with inverted triangles. The approximate extent of the North American ice sheets at 12.9 ka is shown in blue-green, which is consistent with our observations that all sites were ice-free at the time of the YD event.

[Back to Top]

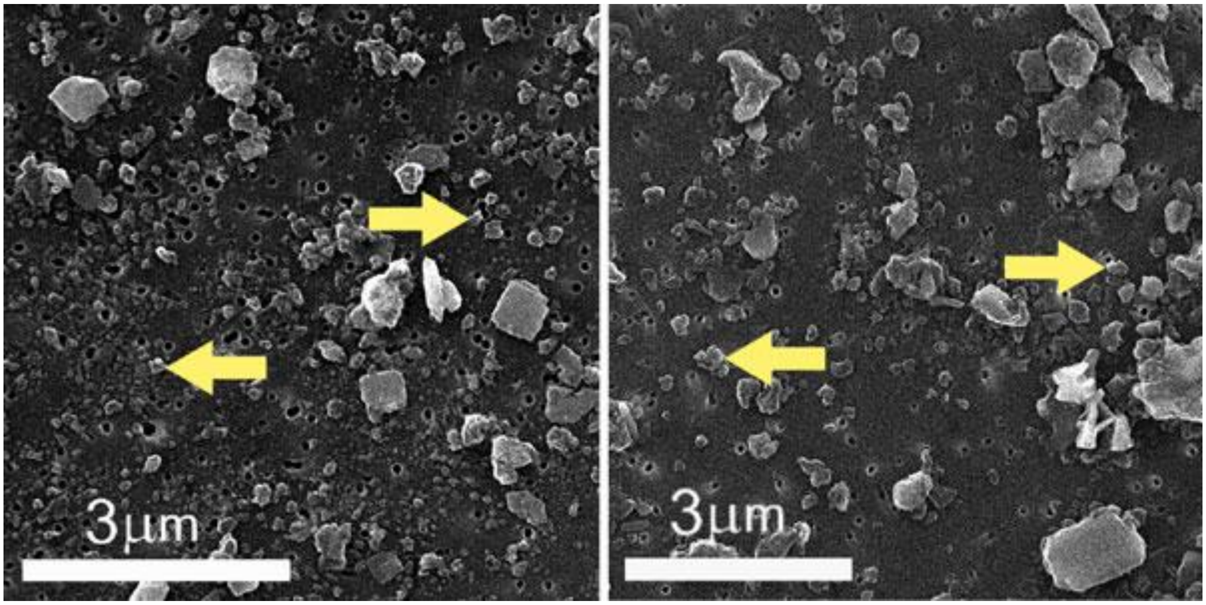

Fig. 10. SEM photomicrographs of mostly individual particles of submicron-sized soot (shown on filter paper at yellow arrows), measured at 1,969 ± 167 ppm from Blackville Bay T13 (*Left*), and measured at 21 ± 7 ppm from Murray Springs (*Right*). The soot levels and morphology from both sites are similar to those from the K/T (1). Only two of eight sites tested exhibited soot, perhaps because of unfavorable conditions for preservation at some sites. Soot was identified using SEM imaging and quantified by particle size analysis and weighing (2).

1. Wolbach WS, Gilmour I, Anders E, Orth CJ, Brooks RR (1988) *Nature* 334:665-9.

2. Wolbach WS, Anders E (1989) *Geochim Cosmochim Acta* 53:1637-1647.

[Back to Top]

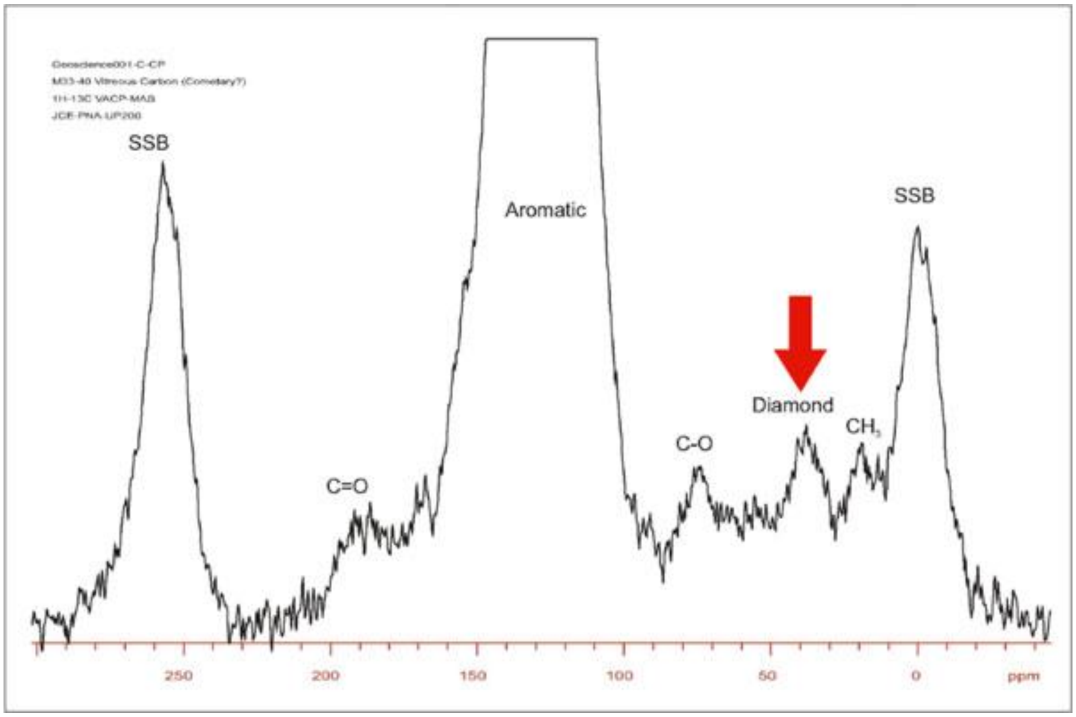

Fig. 11. A ^{13}C NMR spectrum of glass-like carbon from Carolina Bay M33 in Myrtle Beach, South Carolina. This was produced on a Varian Unity-200 NMR spectrometer operating at 50.2 MHz and equipped with a Doty Scientific 7-mm Supersonic MAS probe. Spinning speeds of 6.5 kHz were used and a variable-amplitude, cross-polarization pulse sequence was used with recycle delays of 1 s and a contact time of 1 ms. The aliphatic carbon appears centered at 38 ppm, which is typical of peaks representative of nanodiamonds, where small diamond domains are formed in compressed aromatic/graphitic materials. Of the ≈9-10% aliphatic carbon, the inferred nanodiamond component is estimated to represent ≈3% total carbon.

[Back to Top]

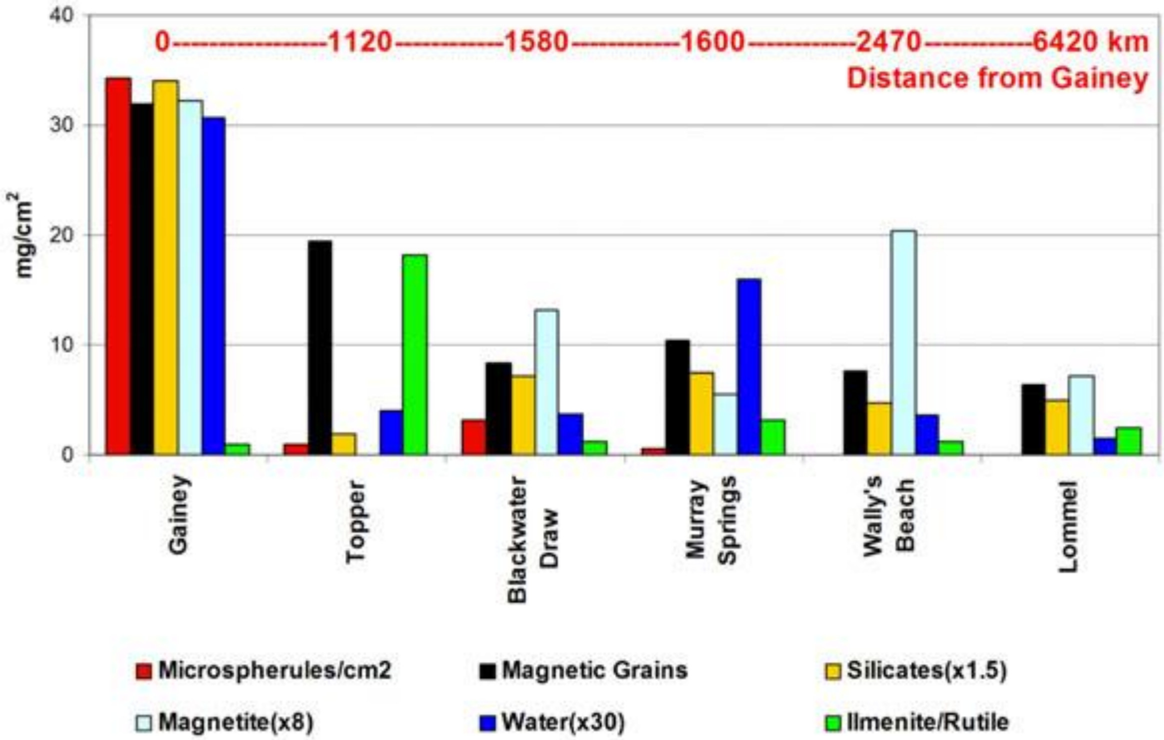

Fig. 12. Deposition rates [calculated by $MG \times D \times \%A \times \pi/100$, where MG (measured in mg/g) is magnetic grain concentration (Table 1), D (in cm) is the YDB layer (Table 1), $\%A$ is percent mineral abundance (Table 2), and π (in g/cm^3) is the average mineral density.] for magnetic microspherules, magnetic grains, and their principal components at YDB sites ordered by distance from the Gainey, MI, site (upper scale). Microspherules, magnetic grains, magnetite, silicates, and water content all dramatically peak at Gainey, suggesting that they are terrestrial products of a nearby impact. Ilmenite/rutile concentrations peak at Topper and are higher than Gainey at all sites, suggesting that they are high-velocity ejecta from an impact. Because magnetic grains at Wally's Beach where recovered from inside an extinct Pleistocene horse skull and may not be representative of the sediment, magnetic grain concentrations there are normalized to those at the nearby Chobot site.

[Back to Top]

Fig. 13. Mammoth bone found with Clovis artifacts (from the Blackwater Draw collection). This bone is stained yellow (arrow) and is highly radioactive (3,000 ppm U) only on the upper side that was just below the black mat. Bones found above or deeper below the black mat are neither stained nor highly radioactive. INAA analysis determined a high U concentration (58 ppm) in YDB sediment at Blackwater Draw, which is ≈10 times the concentration above or below. High U content on fossil bones is due to well known diagenetic processes (1) as confirmed by the corresponding low Th content (<1 ppm) on the stained bone surface. During breakdown of organic material under anoxic conditions, bone beds also may precipitate phosphatic minerals (2), which in turn scavenge and concentrate U. If so, the U enrichment on the bones and in the YDB sediment may have been enhanced by the abundance of bones and other Ca sources in the extinction layer. High levels of radioactivity may, therefore, be potentially useful as an additional diagnostic marker of the YDB layer.

1. Hedges REM (2002) *Archaeometry* 44(3):319-328.

2. Purnachandra Rao V, Naqvi SWA, Dileep Kumar M, Cardinal D, Michard A, Borole DV, Jacobs E, Natarajan R (2000) *Sedimentology* 47(5):945-960.

[Back to Top]

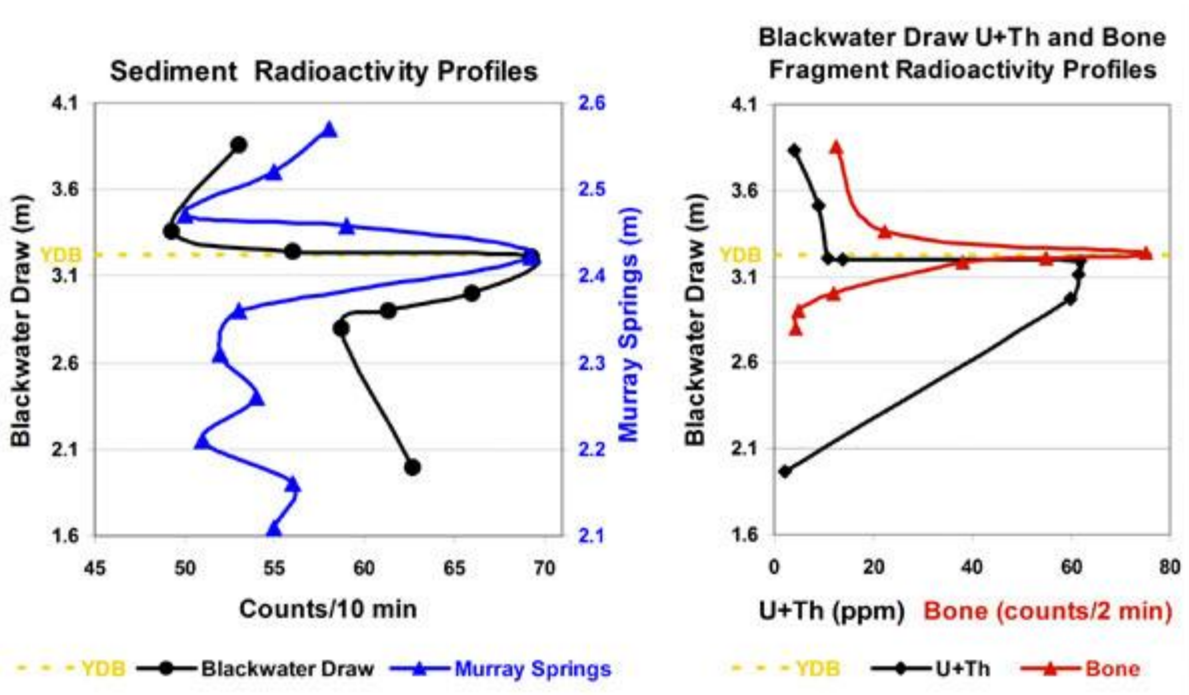

Fig. 14. (*Left*) Radioactivity profiles measured with a Geiger counter at Blackwater Draw and Murray Springs. (*Right*) Radioactivity in bone fragments from Blackwater Draw sediments (1) are compared with U and Th concentrations from Blackwater Draw sediment. Radioactivity peaks in both sediment and bone fragments in the YDB due to high concentrations of U.

1. Fitting J (1963) in *Studies in the Natural Radioactivity of Prehistoric Materials*, eds Jelinek A, Fitting JE (Univ of Michigan, Ann Arbor), pp 66-66.

[Back to Top]

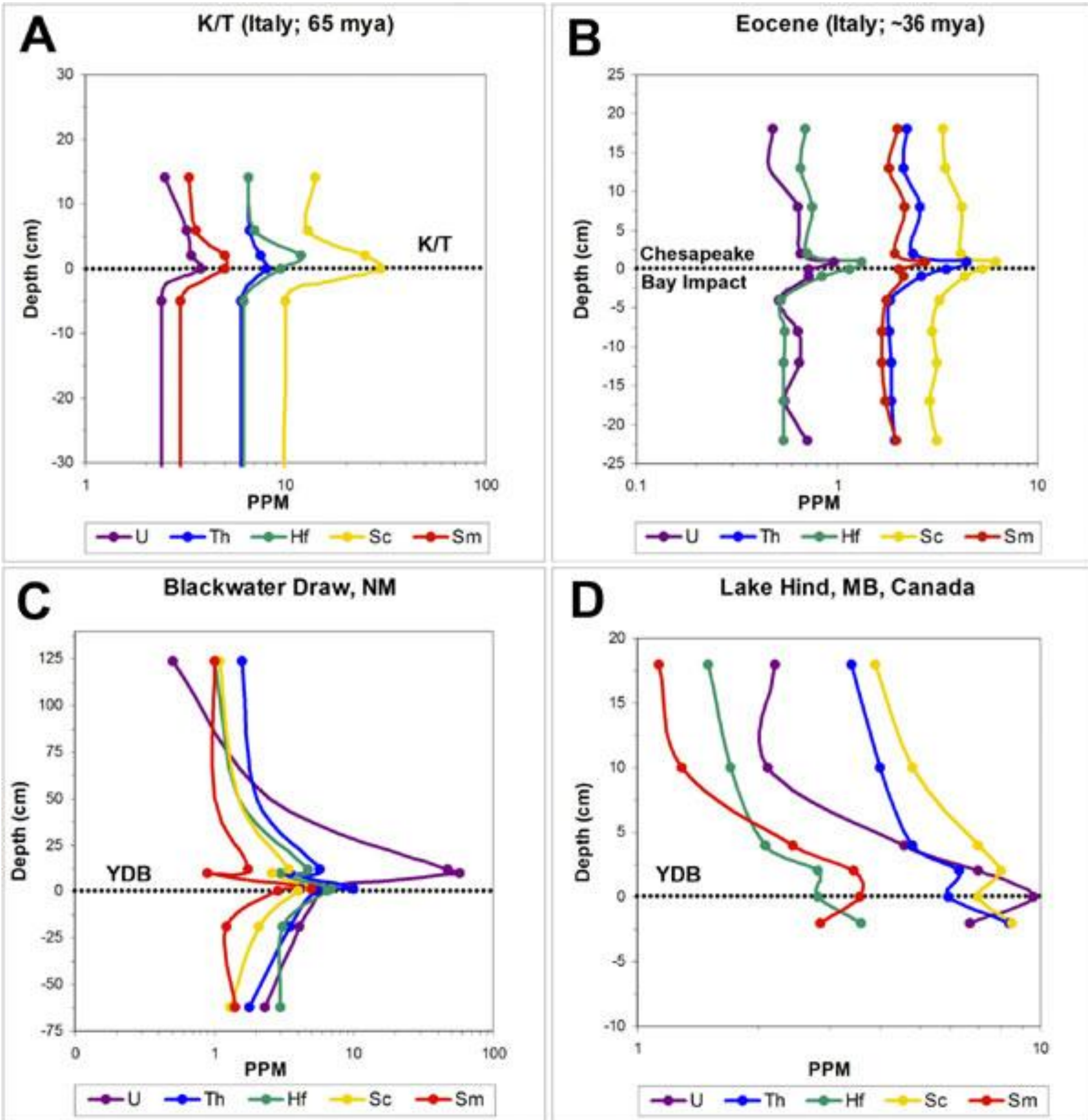

Fig. 15. Sediment concentrations for U, Th, Hf, Sc, and Sm peak in the K/T boundary at Gubbio, Italy (*A*) (1), and the late Eocene Chesapeake Bay impact (≈36 Ma) at Massignano, Italy (2), which produced one of the largest known tektite strewnfields (*B*). (*C* and *D*) Radioactive element concentrations also peak in the YDB at Blackwater Draw, NM, (*C*) and Lake Hind, Manitoba, Canada (*D*). At Blackwater Draw, the uranium increase as determined by INAA is especially large (58 ppm) and yielded the most radioactive sediment analyzed in the study (SI Fig. 14). Concentrations (in ppm) are shown on a log scale, and depth (in cm) is centered on the YDB layer. Ir, Ni, and numerous other elements also peak at the YDB layer (presented in the main text) and are considered to have resulted from impact processes.

1. Alvarez LW, Alvarez W, Asaro F, Michel HV (1980) *Science* 208:1095-1108.

2. Bodiselitsch B, Montanari A, Koeberl C, Coccioni R (2004) *Earth Planet Sci Lett* 223:283-302.

[Back to Top]

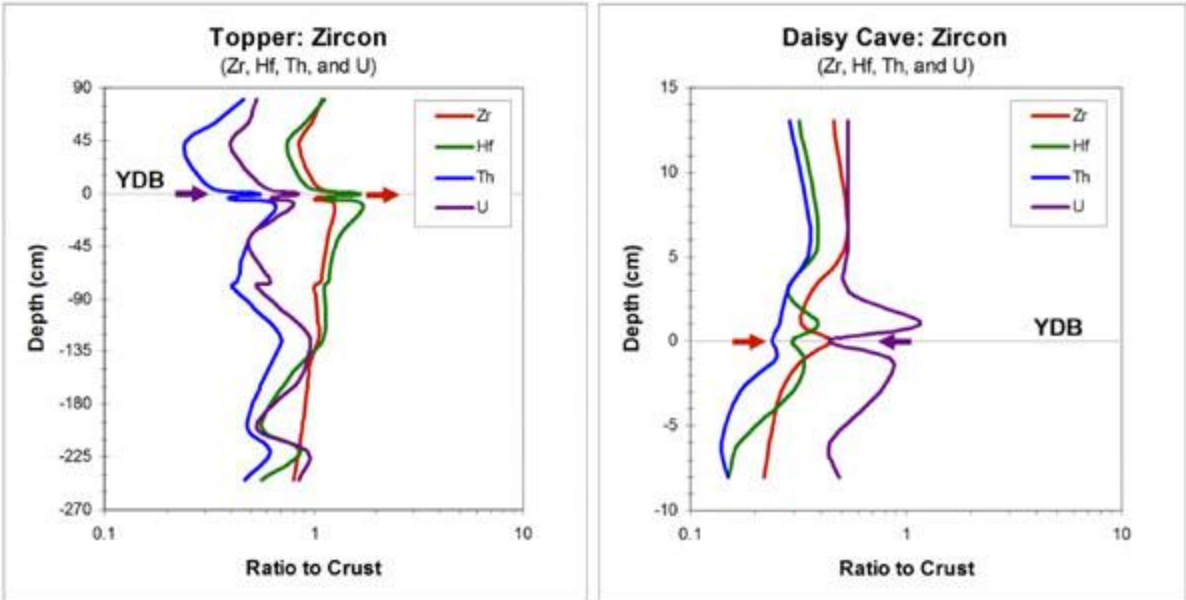

Fig. 16. Zircon ($ZrSiO_4$) is one of several heavy minerals potentially enriched with U and Th that can be concentrated to form a radioactive layer. (*Left*) We analyzed sediment samples at the Topper site for Zr (red arrow), the major constituent of zircon, and found evidence for a minor increase in zircon abundance in the YBD at Topper. When normalized to crustal values, U (purple arrow), Th, and Hf concentrations changed in direct relationship to the abundance of Zr, suggesting that zircon may account for some of the increased radioactivity. (*Right*) In contrast, at Daisy Cave, U decreased relative to zircon, indicating a negative correlation to sediment radioactivity.

[Back to Top]

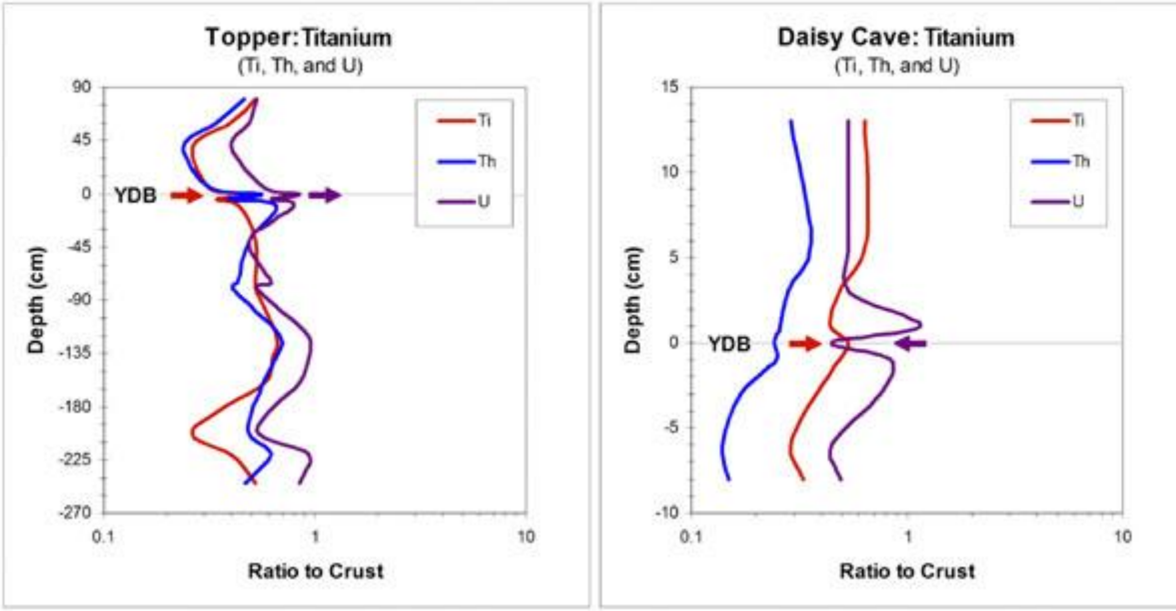

Fig. 17. Ti may appear in the heavy minerals ilmenite, rutile, and titanite. (*Left*) At Topper, the presence of sedimentary Ti (red arrow) correlates well with higher sedimentary levels of U (purple arrow) and Th. (*Right*) However, at Daisy Cave, these relationships were negative, as with zircon. In summary, heavy mineral concentrations tested do not correlate well with an increase in sediment radioactivity at Daisy Cave but do so at Topper, where the formation of lag deposits may have been influenced by the impact. Heavy minerals may be concentrated through impact-related processes such as (*i*) high-velocity winds associated with the shockwave; (*ii*) heavy rains and flooding following the impact; and (*iii*) selective dissolution of sediment by acidic conditions due to fallout and acid rain. However, it is unlikely that lag deposits are typical of the YDB, because these sediment sequences appear to be relatively continuous. Furthermore, such deposits would have concentrated interplanetary dust particles (IDPs), and they would be present in the magnetic fractions isolated from bulk sediments at BWD and Murray Springs. However, these two sites do not show high $^{3}He/^{4}He$ ratios in the magnetic fraction, such as would be present if the lag deposits had concentrated the IDPs, nor does the He in the bulk sediment suggest any such concentration at the boundary. Only the fullerenes concentrate ET He, which is inconsistent with lag deposits and consistent with an impact event at the YDB.

[Back to Top]

SI Text: Research Sites.

Murray Springs. Near Sierra Vista, AZ, Murray Springs is one of several local Clovis mammoth kill-sites associated with a chain of end-Pleistocene ponds at 12.9 ka. Sediments from the YDB layer are mostly fine to coarse fluvial or lacustrine sand. A distinctive black mat, most likely of algal origin, drapes conformably over the bones of butchered mammoths, and a thin layer (<2 cm) that contains YDB markers lies at the base of the black mat and immediately overlies the bones (1). The upper surfaces of some Clovis-butchered mammoth bones, which were in direct contact with the YDB and the black mat, exhibit slightly higher radioactivity and magnetic susceptibility than the lower surfaces.

Blackwater Draw. Blackwater Draw, NM is southwest of the town of Clovis, which gave its name to the type of projectile points first found there. It was a PaleoAmerican hunting site on the bank of a spring-fed waterhole, where the black mat was found draped over bones of butchered mammoths and Clovis artifacts. YDB markers are concentrated in a ≈2-cm layer of fine-grained fluvial or lacustrine sediment that lies at the base of the black mat in the uppermost stratigraphic horizon containing *in situ* mammal bones and Clovis artifacts. The upper surfaces of some mammal bones were in direct contact with the YDB or the black mat and exhibited very high levels of radioactivity. We sampled a 2-m stratigraphic sequence spanning the YDB down into the deep gravels that date to >40 ka and possibly to 1.6 Ma (2). ET markers peaked only in the YDB.

Gainey. North of Detroit, MI, Gainey was a PaleoAmerican campsite located tens of kilometers from the southern margin of the Laurentide Ice Sheet at 12.9 ka. Sediments containing YDB markers are mostly fine alluvial sand and glacial silt. The Gainey site has been closed and hence inaccessible for many years, and only archived samples from the ≈5-cm YDB layer were available for analysis. No black mat was observed.

Wally's Beach. At St. Mary Reservoir, southwestern AB, Canada, Wally's Beach was a stream-fed valley that, at 12.9 ka, supported many species of now-extinct megafauna, including mammoths, camels, and horses. Hundreds of their footprints were found there during prior excavations. A sediment sample of fine-grained and silty alluvium was provided to us by Brian Kooyman from the brain cavity of a horse skull found in the YDB layer amidst Clovis points that tested positive for horse protein, providing some of the first evidence that Clovis peoples hunted horses (3).

Topper. Topper is located on a high bank of the Savannah River near Allendale, SC, and was a Clovis-age flint quarry containing thousands of artifacts. Sediments are eolian, fluvial, colluvial, and alluvial in origin and are comprised mostly of coarse to medium quartz sand. YDB markers occur within a ≈5-cm interval immediately in and above a distinct layer of Clovis artifacts. Lower sediments in the sequence have been dated to >55 ka (4), and no ET markers appear in the stratigraphic sections above or below the YDB. There is no black mat at this site.

At a new excavation, we used the neodymium magnet and a magnetic susceptibility meter to help identify the YD layer based on the high iron content. Shortly afterward, the excavators recovered part of a Clovis point immediately beneath the YD layer, illustrating the usefulness of the YDB markers for locating the Clovis horizon in new locations.

Chobot. Chobot is Southwest of Edmonton, AB, Canada. In Clovis times, it was located along the shore of a proglacial lake, where a supply of quality flint attracted hunter-gatherers. The presence of Clovis artifacts (5) dates this level to an interval of ≈200 yr ending at 12,925 cal B.P. (6). The Clovis level is capped by the YDB layer, above which there is a black mat similar to other sites. The YDB sediment samples are mostly fine-grained and colluvial.

Daisy Cave. A cave/rockshelter on San Miguel Island, Daisy Cave is one of the Channel Islands off the Southern California coast. This cave does not appear to have been occupied until ≈11.5 ka, but a Clovis-age human skeleton was found on nearby Santa Rosa Island, demonstrating that the PaleoAmericans had boats capable of reaching the islands. Several markers were found, but others, including Ir, were not found, possibly because the protected cave shelter prevented accretion. The sediment with YDB markers dates to ≈13.09 ka (7) and varies from fine sand to silt.

Lake Hind. In MN, Canada, Lake Hind was an end-Pleistocene proglacial lake. Various analyses by Boyd *et al.* (8) show that prior to 12.76 ka, the ice dams on the lake failed catastrophically as part of a regional pattern of glacial lake drainages. In this study, we confirmed with calibrated radiocarbon dating that the drainage took place at ≈12.76 ka (UCIAMS 29317). At the YDB, the failure rapidly transformed the lake from deep to shallow water, as shown by pollen analysis and the start of peat accumulation. The sample sediments are fine-grained lacustrine silt and peat.

Morley. Morley is a nonarchaeological site west of Calgary in AB, Canada. The site is on a raised drumlin, a subglacial erosional landform that formed at the end of the Pleistocene during deglaciation (9). The largest drumlin field near Ontario (5,000 km^2) contains 3,000 drumlins that date to shortly after 13 ka, and the age of the Morley drumlin field appears to be similar. Later, the ice sheet melted away leaving atop the drumlin glacial debris containing numerous YDB markers. Samples are mostly gravel grading down through coarse and medium sand.

Lommel. Lommel is described in SI Fig. 8.

***Carolina Bays*.** The Carolina Bays are a group of ≈500,000 highly elliptical and often overlapping depressions scattered throughout the Atlantic Coastal Plain from New Jersey to Alabama (see SI Fig. 7). They range from ≈50 m to ≈10 km in length (10) and are up to ≈15 m deep with their parallel long axes oriented predominately to the northwest. The Bays have poorly stratified, sandy, elevated rims (up to 7 m) that often are higher to the southeast. All of the Bay rims examined were found to have, throughout their entire 1.5- to 5-m sandy rims, a typical assemblage of YDB markers (magnetic grains, magnetic microspherules, Ir, charcoal, soot, glass-like carbon, nanodiamonds, carbon spherules, and fullerenes with ^3He). In Howard Bay, markers were concentrated throughout the rim, as well as in a discrete layer (15 cm thick) located 4 m deep at the base of the basin fill and containing peaks in magnetic microspherules and magnetic grains that are enriched in Ir (15 ppb), along with peaks in charcoal, carbon spherules, and glass-like carbon. In two Bay-lakes, Mattamuskeet and Phelps, glass-like carbon and peaks in magnetic grains (16-17 g/kg) were found ≈4 m below the water surface and 3 m deep in sediment that is younger than a marine shell hash that dates to the ocean highstand of the previous interglacial.

Modern Fires. Four recent modern sites were surface-sampled. Two were taken from forest underbrush fires in North Carolina that burned near Holly Grove in 2006 and Ft. Bragg in 2007. Trees mainly were yellow pine mixed with oak. There was no evidence of carbon spherules and only limited evidence of glass-like carbon, which usually was fused onto much larger pieces of charcoal. The glass-like carbon did not form on oak charcoal, being visible only on pine charcoal, where it appears to have formed by combustion of highly flammable pine resin.

Two surface samples also were taken from recent modern fires in Arizona; they were the Walker fire, which was a forest underbrush fire in 2007 and the Indian Creek Fire near Prescott in 2002, which was an intense crown fire. Trees mainly were Ponderosa pine and other species of yellow pine. Only the crown fire produced carbon spherules, which were abundant (≈200 per kg of surface sediment) and appeared indistinguishable from those at Clovis sample sites. Both sites produced glass-like carbon fused onto pine charcoal.

[Back to Top]

Methods. *Separation of the magnetic fraction from sediment.* Initially, we used the magnet for *in situ* field testing to help locate the peak in grains in the YDB. However, such testing works only under the most favorable conditions, such as in loose, dry sediment with a high concentration of grains. If the samples contain high percentages of clay or are damp, we found that the magnet performs poorly. In addition, even if conditions are ideal but the concentration of grains is low, such as <1g/kg, we found it difficult to quantify the amount of grains on the magnet in the field. In summary, we found it far simpler to locate the YDB by analyzing magnetic grain abundances in the laboratory following the procedures below. We used only grade-42 or higher neodymium magnets, having found that nearly all other magnets are too weak and that some will completely fail to extract any magnetic grains. Typically, we used the size 2 ×1 × 0.5 inches (1 inch = 2.54 cm), which was convenient for field and laboratory work.

Although sonication is a common way to separate magnetic grains, the process was not used in our studies, because the procedure typically collects only the smallest and most magnetic grains, excluding up to 90% of the remainder, including many of the most interesting items, such as titanium-rich microspherules.

Typically, several methods were used to separate magnetic grains from sediment, depending upon the type of sediment. For large-scale processing, the following basic procedures were used with automated equipment and a bank of magnets, which were placed in a moving stream of either wet or dry sediment. Small samples were processed manually.

Loose or sandy sediment. About 500-1,000 g of friable sand or silt was first dehydrated at room temperature and weighed, and then, the samples were put into a container and the lumps were broken up. All of the processing was done using non-metallic tools to avoid adding foreign metal to the sample, and care was taken not to crush the fragile carbon component, if it was to be extracted also. Next, the magnet was placed in a 4-mil plastic bag to prevent grains from sticking directly to the magnet. A sediment sample was poured over the tightly bagged magnet into an empty container. Magnetic grains stuck to the magnet, and when the magnet was removed from the bag, the grains fell into a separate container. The process was repeated until nearly all of the grains were recovered.

Final step. As an essential final step to remove dust and debris, which can conceal the magnetic grains and spherules, the magnetic fraction was placed in a beaker of water. Then, the bagged magnet was gently agitated in the beaker to attract the magnetic grains. These were then deposited on a dry lab dish, by touching the wet bag to the plate after the magnet was removed from the bag. After drying, the sample was weighed, catalogued, and examined microscopically at ×100-150 magnification.

Sticky or clayey sediment. For sediment that was difficult to pulverize, we added ≈4 liters of water to each 500-1,000 g of sediment and homogenized it into slurry. The bagged magnet was then used to extract magnetic grains from the fluidized mixture. The magnetic grains were then released from the magnet into a separate container of water and then retrieved onto a laboratory dish as in the final step discussed above.

Extraction of magnetic microspherules. To find microspherules, the magnetic fraction was extracted from a weighed sediment sample with the neodymium magnet. We found it essential to complete the final step of cleaning the magnetic fraction with water, as outlined above. Also, because there are relatively few microspherules in bulk sediment, it was often necessary to inspect the most or all of the magnetic fraction extracted from 500-1,000 g of sediment. Next, one or more ≈100 mg aliquots of the magnetic fraction were weighed, dusted sparsely across a microscope slide, and scanned microscopically. Microspherules, which typically ranged from 10-100 μm, were counted, and abundances were extrapolated to quantity per kg. While viewed at ×100-150 magnification, selected microspherules were removed from the magnetic fraction manually with a moistened probe and placed onto an SEM mount or double-sided tape on a microscope slide. These spherules were either left whole or sectioned and given a microprobe polish for analysis by laser ablation or x-ray fluorescence (SEM/XRF).

Extraction of carbon spherules, glass-like carbon, and charcoal. Carbon spherules have a low specific gravity, and water floatation was used to assist with their separation. Typically, one kg of sample was added to ≈4 liters of water and agitated. The floating fraction was captured with a 150-μm sieve. In addition, there was often a carbon fraction with a specific gravity slightly higher than that of water, and that was removed from the top of the wet sediment visually. After drying at low temperatures, the carbon spherules were collected either visually or gravimetrically by vibrating the dried sample on an inclined, polished surface. Glass-like carbon and charcoal, contained in the same sample, were extracted manually and weighed.

Radiocarbon. AMS radiocarbon dating was performed by J. Southon (Keck Carbon Cycle AMS Facility) on peat and silt from Lake Hind. The radiocarbon date was converted to calibrated dates using IntCal04 (11).

Inductively coupled plasma mass spectrometry (ICP-MS) analysis. *ICP-MS analyses*. The isotopes evaluated for this investigation were: $^{52,53}Cr$; $^{58,60,61,62,64}Ni$; and $^{191,193}Ir$. Uncertainties varied by isotope, but all were less than ±20%. These isotopes were selected to evaluate the possibility of ET material in the sediment samples. Only Ir showed anomalous values. More details on the rationale for the selection of these isotopes, the ICP-MS conditions, analytical details of other isotopes not reported here, and the results and basis of the elements selected for further study will be presented in a forthcoming paper. This suite of isotopes allowed the use of aqua regia type acid mixtures to facilitate digestions. The digestion scheme allowed elements on the outside versus inside of the particles to be studied separately.

The analysis process involved digestion with concentrated Fisher OPTIMA nitric acid (HNO_3) and then concentrated Fisher OPTIMA hydrofluoric acid (HF) with evaporation of the hydrofluoric acid before ICP-MS analysis in 5% (vol/vol) HNO_3. All vessels and containers were acid washed in 10% nitric acid overnight, rinsed with ASTM I water, and dried beforehand.

Digestions. Initially, large sample weights of ≈100 g were used to screen the various isotope ratio changes to detect changes in uranium (U) isotopes. A method blank and a positive control (National Institutes of Standards and Technology, Buffalo River Sediment SRM 8704) were analyzed in parallel.

Screening digestions. Each 100-g sample ground in a mortar and pestle to pass through a 149-μm sieve was allowed to digest overnight in 75 ml of concentrated nitric acid in a Teflon beaker of known weight in a fume hood. The temperature on a hot plate was stepped-through for 2 h with Teflon watch glasses on at 50-55°C, 70-75°C, 80-85°C, 90-95°C, 100-105°C, and 110-115°C and then allowed to reflux with Teflon watch glasses until there were no more brown fumes. The gradual ramp was necessary to avoid boil-over and bumping of the heterogeneous digestion mixture. This took up to a week. After cooling, 75 ml of concentrated HF was added and allowed to stop bubbling. After 2 h, the above temperature ramp was repeated with watch glasses on after adding another 45 ml HF. The watch glasses were removed and the 2 h temperature steps then done at 125-130°C, 135-140°C, 145-150°C, 165-170° C, 175-180°C, and 195-200°C until dry. After cooling, the residue was weighed, and broken up with an acid washed pestle/Teflon spatula. The same process was repeated on the residue with 60 ml of concentrated HF alone, and then another 60 ml.

The dried broken up digestion residue (usually between 36% and 78% of the original weight) was extracted with 5% nitric acid in 2-h steps at 50°C, with each liquid being combined by decantation after cooling in a small 150-ml Teflon beaker where the combined dilute nitric acids extractions were evaporated at 110-115°C. This amalgamate was evaporated to ≈15 ml and used for analysis after cooling. This solution had a precipitate after standing and the liquid portion was carefully decanted into another centrifuge tube that was then centrifuged at 900 × *g*. The solids of the dilute HNO_3 extraction steps and the centrifugation step were combined, dried to constant weight, and set aside for further analysis by nondestructive analytical chemistry techniques. This residual material was ≈27-64% of the original weight. The centrifuge tube supernatant was analyzed by ICP-MS, and its dry weight was ≈3.5-5.6% of the original weight. The solutions were yellow, orange, or red to orange compared to colorless for the method blank, and orange for the NIST sediment sample.

After the initial screening results were analyzed, small amounts of samples of 1 g were then digested to provide a HNO_3/HCl available fraction, a HF available fraction after nitric acid digestion, and a residual fraction.

Small-weight digestions. Approximately 1 g of the sample ground in a mortar and pestle to pass through a 149-µm sieve was digested twice in a Teflon beaker with concentrated HNO_3 (30 ml at room temperature for 16 h, 55-60°C for 16 h, 85-90°C for 16 h, then 135-140°C for 16 h before cooling and decanting the supernatant into another Teflon beaker, followed by 20 ml of concentrated nitric acid digestion for 16 h at 135-140°C) followed by three digestions with 4:1 HCl/HNO_3 (20 ml × 3, each for 16 h at 135-140°C). Each residue with solids was dried at 135-140°C before the next digestion (SR1). The final solid residue after the last 4:1 HCl/HNO_3 leaching was also retained. The 5 extractions were combined, evaporated, and the dry broken up residue leached with 30 ml 5% (vol/vol) nitric acid at 100°C to constitute the soluble phase that was centrifuged for 10 min at 900 × *g*. The solid residues (from leaching with 5% nitric acid and centrifugation) were combined with SR1 for the HF digestions

Two HF digestions followed, one with 4:1 HF/HNO_3 (one with 30 ml for 16 h at room temperature, 55-60°C for 16 h, and then 135-140°C for 16 h) and decanting the supernatant into another Teflon beaker. The second digestion of the dried residue with particulates was with 30 ml of concentrated HF, and the second leaching was combined with the first extraction, dried, and the solid then leached with 5% nitric acid, and the leachate centrifuged. The centrifugation solids and leachate solids were combined with the solid from the second HF digestion step and then dried. The Teflon beakers were then scraped with a Teflon spatula to provide the residual solid weight that varied from 0.02% to 10% of the original weight. These residues were further analyzed by nondestructive instrumental analysis. The colors of these residual solids varied from black/greasy and black/hard to white flake (samples) to yellow-orange/cream (method blank and the National Institute of Standards and Technology sample). The digestion of small samples was thus at least 90% efficient in digesting the original sample.

X-ray Fluorescence (XRF). Representative microspherules were sliced, polished, and mounted for analysis by XRF with a scanning electron microscope (SEM) by B. Cannon (Cannon Microprobe). The x-ray spectra were obtained using an ARL SEMQ Electron Microprobe operated at 20 kV accelerating voltage, 50-nA beam current, 52.5° x-ray take off angle, a Kevex 2003 energy dispersive x-ray detector (EDS) biased at 620 V with an 8-µm-thick beryllium window and a PGT *MCA 4000* multichannel analyzer. The resolution of the detector is 159 eV at Mn K alpha. Elements with atomic number 10 and smaller are not detected by this system due in part to thickness of the beryllium window on the detector. Different regions of the microspherules were randomly analyzed to obtain average elemental concentrations.

Prompt gamma-ray activation analysis (PGAA). PGAA of samples from many sites was performed at the Department of Nuclear Research, Institute of Isotopes in Hungary. PGAA is a non-destructive technique (12), using neutron beams to excite the samples producing gamma-ray spectra unique to each element. Typically, several gamma-rays are excited for each element, which can be used for analysis. PGAA is sensitive to the main constituents, except oxygen, and many trace elements in a sample. Concentrations are normalized to the total sample composition assuming standard oxidation states. Bulk samples of magnetic grains and microspherules, ranging in size from 9 mg to 13 g were analyzed with PGAA for H, B, F, Na, Al, S, Si, Mg, Cl, K, Ca, Sc, Ti, V, Cr, Mn, Fe, Co, Ni, Cu, Cd, Sm, Eu, and Gd. Uncertainties varied by element, but all were less than ±20%.

Nneutron activation analysis (NAA). The analysis of samples from many sites was performed at Becquerel and Activation Laboratories in Canada and at the Department of Nuclear Research, Institute of Isotopes, in Hungary. NAA was used to analyze trace element concentrations in both bulk sediment and magnetic grain samples, which were analyzed for Na, Si, Ca, Sc, Cr, Fe, Co, Zn, As, Se, Br, Rb, Zr, Mo, Ag, Cd, Sn, Sb, Te, Cs, Ba, Ce, La, Nd, Sm, Eu, Tb, Yb, Lu, Hf, Ta, W, Ir, Au, Hg, Th, and U. Uncertainties varied by element, but all were less than ±20%.

1. Haynes CV, Jr. (2007) in *Murray Springs: A Clovis site with Multiple Activity Areas in the San Pedro Valley, Arizona*, eds, Haynes CV, Jr, Huckell BB (Univ of Arizona Press, Tucson), pp 240-249.

2. Haynes CV (1995) *Geoarchaeology* 10(5):317-388.

3. Kooyman B, Newman ME, Cluney C, Lobb M, Tolman S, McNeil P, Hills LV (2001) *Am Antiq* 66:686-691.

4. Goodyear A (2005) In *Paleoamerican Origins: Beyond Clovis*, eds Bonnichsen R, Lepper BT, Stanford D, Waters MR (Texas A&M Univ. Press, College Station), pp 113-132.

5. Editor. (2000) *Mammoth Trumpet* 16(1):1-4.

6. Waters MR, Stafford TW, Jr (2007) *Science* 315:1122-1126.

7. Erlandson J, Kennett DJ, Ingram BL, Guthrie DA, Morris DP, Tveskov M, West GJ, Walker P (1996) *Radiocarbon* 38:355-373.

8. Boyd M, Running GL, Havholm K (2003) *Geoarchaeology* 18(6):583-607.

9. Boyce JI, Eyles N (1991) *Geology* 19:787-790.

10. Sharitz RR, Gibbons JW (1982) *The Ecology of Southeastern Shrub Bogs (Pocosins) and Carolina Bays: A Community Profile* (U.S. Fish and Wildlife Ser, Washington, DC), pp 93-94.

11. Stuiver M, Reimer PJ (1993) *Radiocarbon* 35:215-230.

12. Molnar GL, ed (2004) *Handbook of Prompt Gamma Activation Analysis* (Kluwer Academic, Boston, MA), pp 423.

[Back to Top]

Table 2. Youngest dates available for the sites examined containing YDB markers

YDB test sites	No. of dates	Black mat	Cal. B.P.	± (1σ)	^{14}C Date	± (1σ)	Source
Blackwater Draw, NM	1	Yes	12982	575	11040	500	Ref. 1
Chobot, AB, CAN	1	Yes	≈13000	—	Archaeology	—	Ref. 2
Daisy Cave, CA	1	Yes	13090	140	11180	130	Ref. 3
Gainey, MI	1	No	12400	1000	TL	—	Ref. 4
Lake Hind, MB, CAN	1	Yes	12755	87	10610	25	UCIAMS 29317
Lommel, Belgium	1	Yes	12943	30	10950	50	Ref. 5
Morley, AB, CAN	1	Yes	≈13000	—	Deglaciation	—	Ref. 6
Murray Springs, AZ	8	Yes	12916	25	10890	50	Ref. 1
Wally's Beach, AB, CAN	1	No	12966	61	10980	80	Ref. 7
Weighted average			**12938**	**25**			

In most cases, the sites were independently dated by other researchers, as noted under "Source," and were calibrated by the authors using IntCal04 (8). Two sites were not previously radiocarbon dated: (*i*) Morley drumlin is constrained by the end of local deglaciation to ≈13 ka; and (*ii*) the Chobot site is of Clovis age because of an abundance of Clovis artifacts, limiting the site's age, according to Waters and Stafford (9), to a minimum range of ≈200 years between 13,125 to 12,925 cal. B.P. The average calibrated age of all sites analyzed is 12938 ± .25 B.P., which agrees closely with the GISP2 date of 12.9 ka (see SI Fig. 6). Seven of the 10 sites exhibit a black mat immediately overlying the YDB layer.

1. Taylor RE, Haynes CV, Stuiver M (1996) *Antiquity* 70:515-525.
2. Ana (2000) *Mammoth Trumpet* 16(1):1-4
3. Erlandson J, Kennett DJ, Ingram BL, Guthrie DA, Morris DP, Tveskov M, West GJ, Walker P (1996) *Radiocarbon* 38:355-373.
4. Simons DB, Shott MJ, Wright HT (1984) *Arch East N Am* 12:266-267.
5. Van Geel B, Coope GR, Vander Hammen T (1989) *Rev Paleont Palyn* 60:25-129.
6. Boyce JI, Eyles N (1991) *Geology* 19:787-790.
7. Kooyman B, Newman ME, Cluney C, Lobb M., Tolman S, McNeil P, Hills LV (2001) *Am Antiq* 66:686-691.
8. Stuiver M, Reimer PJ (1993) *Radiocarbon* 35:215-230.
9. Waters, MR, Stafford TW, Jr (2007) *Science*, V 315:1122-1126.

[Back to Top]

Table 3. Summary of Ir measurements in and around the YDB

	Depth	Magnetic Grain Concentration, ppb					Bulk Sediment Concentration, ppb			
Interval and site	**(cm)**	**Actlabs**	**UCLA**	**Becquerel**	**VUB**	**Budapest**	**Actlabs**	**UCLA**	**Becquerel**	**VUB**
YDB layer										
Gainey	20	—	<0.1	<2	—	—	<1	<0.6	<0.5 (3)	—
Murray Springs	246-247	<1	<0.1	<11 (2)	—	<6	≈**2.2**,<1	<0.6	<0.5 (3)	—
Blackwater Dr	263-272	**24±5**	—	<6 (2)	—	—	≈**2.2**,<0.1 (3)	—	<50	<0.5
Chobot	12-15	—	—	<100	—	—	—	—	—	—
Morley Drumlin	30	—	<0.1	<100	—	—	—	—	—	—
Wally's Beach	5	—	**51±8**	<100	—	—	<1	—	<50	—
Lake Hind	26-30	—	—	—	—	—	≈**2.2**,≈**3.8**	≈**0.4**,≈**0.7**	—	—
Lommel	40-44	**117±12**	≈**0.5**	—	—	<5	<1 (2)	—	—	—
Daisy Cave	100	—	—	—	—	—	<1	—	—	—
Topper	75-85	≈**2.8**	—	<100 (2)	—	—	<1 (4)	—	<50 (3)	—
Black Mat layer										
Murray Springs	245	—	—	—	—	—	—	—	<5	—
Blackwater Dr	252-263	—	—	—	—	—	≈**2.0**,<1	—	<5	<0.5
Lake Hind	26	—	—	—	—	—	≈**3.0**	≈**0.6**	—	—
Carolina Bays										
Blackville Bay	0-240	**15±3**	≈**0.5**	<100 (2)	—	—	**4±2**,<0.5 (6)	—	<0.5 (4)	—
Bladen Bay-B14	20-100	—	—	<100	—	—	—	—	<100 (2)	—
Myrtle Bay-M33	0-700	≈**2.1**<0.5 (4)	—	<5 (3)	—	—	≈**0.5**,<0.5 (7)	—	<50 (4)	—
Howard Bay	325-594	**15±3**,<1 (5)	—	—	—	—	—	—	—	<0.5
Non-YDB layers										
Murray Springs	0	<1	<0.1	<5	—	—	—	—	—	—
	216	—	—	—	—	—	—	<0.1	—	—
	248-262	—	—	—	—	—	—	<0.1	<5 (2)	—
Blackwater Dr	140-252	—	—	<50	—	—	<0.1 (2)	—	<5 (2)	—
	283-468	—	—	<2	—	<6	<0.1 (4)	—	<5 (2)	<0.5
Chobot	8	—	—	—	—	—	<1	—	—	—
Lake Hind	12-20	—	—	—	—	—	<1 (2)	—	—	—
	32	—	—	—	—	—	<1	—	—	—
Lommel	30	—	—	—	—	—	<1	—	—	—
	48-70	<7	—	—	—	—	<1 (3)	—	—	—
Daisy Cave	56-96	—	—	—	—	—	<1(6)	—	—	—
	104-108	—	—	—	—	—	<1(2)	—	—	—
Topper	0-40	—	—	<26(2)	—	—	<1	—	<5(2)	—
	120-325	<0.5	—	<27 (7)	—	—	<1 (4)	—	<5 (7)	—

Neutron Activation Analysis (NAA) measurements were performed at Actlabs and Becquerel Laboratories in Canada, and by Andras Simonits at the Budapest Reactor. ICP-MS measurements were performed by S.S. Que Hee at the University of California, Los Angeles (UCLA), and by P. Claeys at Vrije Universiteit Brussel (VUB). If more than one lower limit was measured, the lowest limit is given and the total number of measurements is shown in parentheses. Positive results, indicated in boldface type, were observed only in the YDB magnetic grains (5 of 21 measurements), YDB bulk sediments (6 of 33 measurements), the black mat (3 of 7 measurements), and in Carolina Bay magnetic grains (4 of 19 measurements) and Bay bulk sediments (2 of 25 measurements). The grand total was 20 positive out of 105 measurements. Above and below the YDB, no Ir was observed in 62 measurements of magnetic grains (17 measurements) and sediments (45 measurements). The large variation in Ir concentrations at various sites is attributed to the nugget effect (1), resulting from small sample sizes, and to the fact that many concentrations were near the lower NAA detection limit of 1-2 ppb. All 20 positive Ir measurements were substantially above crustal abundance (0.020 ppb). Uncertainties for positive values are ±90%, unless otherwise noted.

1. Meisel T, Moser J, Wegscheider W (2001) *Fresenius' J Anal Chem* 370:566-572.

[Back to Top]

Table 4. Summary of YDB markers found at the sites as discussed in this paper

Sites	Latitude—Longitude	Magnetic grains, g/kg	Magnetic spherules, # per kg	Glass-like carbon g/kg	Carbon spherules # per kg	Charcoal, g/kg	3He R/Rair fullerenes* Avg (max)	Carbon soot, ppm	Black mat	Ir, max. ppb
CLOVIS SITES (with artifacts)										
Blackwater Draw, NM	34.27564N 103.32633W	2.14	768	0.03	No	0.03	3 (11)	No	Yes	24
Chobot, AB, CAN	52.99521N 114.71773W	1.92	578	0.11	11	0.19	—	No	Yes	No
Gainey, MI	42.93978N 83.72111W	3.20	2144	0.08	1232	0.12	—	—	No	No
Murray Springs, AZ	31.57103N 110.17814W	2.62	109	0.03	No	0.06	29 (87)	21	Yes	2.2
Wally's Beach, AB	49.34183N 113.15440W	7.79	6	—	—	—	—	—	No	51
Topper, SC (T1)	33.00554N 81.49001W	0.51	—	0.06	257	No	—	—	No	2.8
Topper, SC (T2)	33.00545N 81.49056W	1.95	97	0.07	—	No	—	—	No	No
CLOVIS-AGED SITES										
Daisy Cave, CA	34.04207N 120.32009W	Yes	Yes	Yes	Yes	Yes	81 (108)	No	Yes	No
Lake Hind, MB, CAN	49.43970N 100.69783W	0.28	No	0.22	184	Yes	—	No	Yes	3.0
Lommel, Belgium	51.23580N 5.26403E	0.75	16	0.06	No	0.13	—	No	Yes	117
Morley drumlin, AB	51.14853N 114.93546W	9.90	1020	Yes	16	0.06	—	—	Yes	No
CAROLINA BAYS (with paleosol beneath)										
Blackville, SC (T13)	33.36120N 81.30440W	2.8	205	0.03	803	0.03	—	1969	No	15
Myrtle Bch, SC (M31)	33.83776N 78.69565W	0.86	36	0.21	492	0.73	—	—	No	No
Howard Bay, NC (HB	34.81417N 78.84753W	1.27	22	0.01	1458	2.12	—	—	No	15
Lk Mattamuskeet, NC	35.51865N 76.267917W	16.12	—	.007	No	Yes	—	—	No	No
CAROLINA BAYS (no paleosol reached)										
Myrtle Bch, SC (M33)	33.81883N 78.74181W	0.45	20	16.25	142	Yes	84 (682)	No	No	2.1
Myrtle Bch, SC (M24)	33.83118N 78.72379W	—	—	Yes	Yes	Yes	—	—	No	No
Myrtle Bch, SC (M32)	33.84034N 78.70906W	—	—	Yes	Yes	Yes	—	—	No	No
Salters Lake, NC (B14)	34.70992N 78.62043W	0.53	42	0.42	777	0.20	—	—	No	No
Lumberton, NC (L33)	34.75566N 79.10870W	0.08	—	0.14	Yes	Yes	—	—	No	No
Lumberton, NC (L28)	3477766. N 79.05008W	—	—	Yes	Yes	Yes	—	—	No	No
Lumberton, NC (L31)	34.78117N 79.04774W	—	—	Yes	Yes	Yes	—	—	No	No
Lumberton, NC (L32)	34.79324N 79.01871W	—	—	Yes	Yes	Yes	—	—	No	No
Moore County, NC	35.30104N 78. 84753W	0.91	—	0.02	152	11.63	—	—	No	No
Sewell, NC	34.95800N 78.70280W	—	—	0.11	126	0.03	—	—	No	No
Lake Phelps, NC	35.78412N 76.434383W	17.10	—	0.013	No	Yes	—	—	No	No
AVERAGES		3.4	389	0.99	489	1.39	49 (222)	995		

*The first value is the total He (as R/R_{air}) released at all temperatures. max. indicates the highest ratio measured for ET He (He as R/R_{air}) during step-heating of the fullerenes or acid-resistant residue.

[Back to Top]

Table 5. XRF analysis of magnetic (mag.) microspherules from the

YDB layers at Blackwater Draw, Gainey, and Morley drumlin

Site-Sample	MgO	Al_2O_3	SiO_2	CaO	TiO_2	MnO	FeO	Ni
Blackwater Draw-1	1.9	3.7	5.8	—	13.0	1.7	73.9	—
Blackwater Draw-2	0.8	2.3	3.1	—	53.1	3.5	37.2	—
Gainey-1	—	2.7	5.1	—	—	—	92.2	0.02
Gainey-2	—	24.8	55.0	—	2.0	—	18.2	—
Gainey-3	—	2.9	4.0	—	68.1	0.1	24.9	—
Gainey-4	—	6.4	40.1	21.3	25.4	—	6.9	—
Gainey-5	—	1.9	3.7	—	29.2	1.0	64.2	—
Morley-1	—	2.7	4.5	—	47.3	1.7	43.9	—
Morley-2	1.8	3.0	4.6	—	40.3	—	50.3	—
Morley-3	—	1.7	1.9	—	—	—	84.3	12.1*
Morley-4	—	3.4	11.5	1.3	—	—	83.9	—
Lommel-1	—	—	—	—	74	—	16	—
Lommel-2	—	—	—	—	54	—	11	—
Lommel-3	—	—	—	—	74	—	16	—
Microspherule average	0.4	5.0	12.7	2.1	25.3	0.7	52.7	1.1*
Mag. grains average†	1.5	4.7	36	2.1	20.5	1.4	31	0.01
Crustal average (ref. 1)	2.5	15	67	3.6	0.6	0.1	5	0.005

The YDB microspherules are enriched in titanium and comparable to magnetic grains from the Blackwater Draw, Murray Springs, Topper, and Lommel sites. Microspherules and magnetic grains are very similar to each other in composition, suggesting a similar source. On the other hand, both are very different from average crustal abundances. All values are in percentage of total weight with uncertainties of less than ±20%.

*The Morley drumlin microspherules were possibly derived from a broad area of ice-sheet melting and the atypically high-Ni concentration may indicate that this spherule does not date to the YDB.

† Average of values from Blackwater Draw, Murray Springs, Topper, and Lommel.

1. Rudnick R, Gao R (2003) Vol 3, *Treatise on Geochemistry,* eds Holland H, Turekian K (Elsevier, Oxford), pp 1-64.

[Back to Top]

View publication stats